

**A REVERSE OSMOSIS TREATMENT PROCESS FOR PRODUCED WATER:  
OPTIMIZATION, PROCESS CONTROL, AND RENEWABLE ENERGY  
APPLICATION**

A Thesis

by

**BRETT MARETH**

Submitted to the Office of Graduate Studies of  
Texas A&M University  
in partial fulfillment of the requirements for the degree of

**MASTER OF SCIENCE**

August 2006

Major Subject: Chemical Engineering

**A REVERSE OSMOSIS TREATMENT PROCESS FOR PRODUCED WATER:  
OPTIMIZATION, PROCESS CONTROL, AND RENEWABLE ENERGY  
APPLICATION**

A Thesis

by

**BRETT MARETH**

Submitted to the Office of Graduate Studies of  
Texas A&M University  
in partial fulfillment of the requirements for the degree of

**MASTER OF SCIENCE**

Approved by:

Chair of Committee,	Maria Barrufet
Committee Members,	Roy Hann
	John Baldwin
Head of Department,	Kenneth Hall

August 2006

Major Subject: Chemical Engineering

**ABSTRACT**

A Reverse Osmosis Treatment Process for Produced Water: Optimization, Process Control, and Renewable Energy Application. (August 2006)

Brett Mareth, B.S., Texas A&M University

Chair of Advisory Committee: Dr. Maria Barrufet

Fresh water resources in many of the world's oil producing regions, such as western Texas, are scarce, while produced water from oil wells is plentiful, though unfit for most applications due to high salinity and other contamination. Disposing of this water is a great expense to oil producers. This research seeks to advance a technology developed to treat produced water by reverse osmosis and other means to render it suitable for agricultural or industrial use, while simultaneously reducing disposal costs. Pilot testing of the process thus far has demonstrated the technology's capability to produce good-quality water, but process optimization and control were yet to be fully addressed and are focuses of this work. Also, the use of renewable resources (wind and solar) are analyzed as potential power sources for the process, and an overview of reverse osmosis membrane fouling is presented.

A computer model of the process was created using a dynamic simulator, Aspen Dynamics, to determine energy consumption of various process design alternatives, and to test control strategies. By preserving the mechanical energy of the concentrate stream of the reverse osmosis membrane, process energy requirements can be reduced several fold from that of the current configuration. Process control schemes utilizing basic feedback control methods with proportional-integral (PI) controllers are proposed, with the feasibility of the strategy for the most complex process design verified by successful dynamic simulation. A macro-driven spreadsheet was created to allow for quick and easy cost comparisons of renewable energy sources in a variety of locations. Using this tool, wind and solar costs were compared for cities in regions throughout Texas. The renewable energy resource showing the greatest potential was wind power, with the analysis showing that in windy regions such as the Texas Panhandle, wind-generated power costs are approximately equal to those generated with diesel fuel.

## ACKNOWLEDGEMENTS

I would like to express my appreciation to the many who have given of their time and consideration in helping me carry out this research. Foremost thanks to Dr. Maria Barrufet, my Advisor, for her helpful ideas, encouragement, and patience in guiding me through the research process.

I would like to thank Dr. John Baldwin and Dr. Roy Hann for serving on my committee and for providing their valuable time.

Special thanks to Mr. Jerry Bradshaw for his sound advice on control system design, Dr. Juergen Hahn for his input on controls and dynamic simulation, and for the many who helped me through frustrating difficulties in learning to use the simulator, including Srinivasan Rajaraman, Babatunde Oyekan, Dr. Baldwin, and the support personnel at AspenTech. My gratitude also goes out to all of the others who I am failing to mention by name, but who have made valuable contributions as well.

## TABLE OF CONTENTS

	Page
ABSTRACT .....	iii
ACKNOWLEDGEMENTS .....	iv
TABLE OF CONTENTS .....	v
LIST OF FIGURES .....	vii
LIST OF TABLES .....	viii
1. INTRODUCTION.....	1
1.1    Significance and Objectives .....	1
1.2    Historical Perspective.....	3
2. THEORY AND LITERATURE REVIEW.....	6
2.1    Membrane Basics .....	6
2.2    Measure of Membrane Performance .....	8
2.3    Membrane Fouling .....	12
2.4    Literature Survey: Treatment of Produced Water .....	13
2.5    Renewable Energy and Applications to Desalination Processes .....	14
2.6    Dynamic Simulation and Control System Design.....	20
3. PROCESS DESCRIPTION AND DESIGN ALTERNATIVES .....	23
3.1    Existing Design .....	23
3.2    Alternative Designs .....	24
4. COMPUTER SIMULATION AND CONTROL SYSTEM DESIGN .....	27
4.1    Methodology .....	27
4.2    Simulation Results.....	38
5. EVALUATION OF POTENTIAL RENEWABLE ENERGY USE .....	48
5.1    Diesel Generation .....	48
5.2    Renewable Sources .....	50
6. CONCLUSIONS AND RECOMMENDATIONS.....	57
REFERENCES .....	59
APPENDIX A .....	64
APPENDIX B .....	69

	Page
APPENDIX C .....	70
APPENDIX D .....	75
VITA .....	77

## LIST OF FIGURES

FIGURE	Page
1. Dead-End and Cross Flow Filtration.....	6
2. Membrane Separations Spectrum.....	7
3. Spiral-Wound Membrane .....	8
4. Concentration Polarization .....	11
5. Weibull Distribution.....	18
6. Possible Process Configurations .....	25
7. Aspen Dynamics Plot .....	29
8. Membrane Pressure Drop.....	31
9. Energy Consumption Comparison .....	39
10. Energy Consumption, Various Feed Fluxes.....	40
11. Original / Series Control System.....	43
12. Pressurized Recycle Control System.....	44
13. Finding Ultimate Gain.....	47
14. After Z-N Tuning .....	47
15. U.S. Diesel Retail Prices .....	49
16. Renewable Energies Spreadsheet.....	52
17. Solar Energy Costs .....	54
18. Wind Energy Costs.....	55
19. Texas Solar Resource Map.....	75
20. Texas Wind Speed Map .....	76

**LIST OF TABLES**

TABLE	Page
1. Mixer (High-Pressure Tank) Parameter Settings .....	34
2. Separator (RO Membrane) Parameter Settings .....	35
3. Streams Parameter Settings .....	35
4. Energy Consumption, Series Configuration.....	41
5. Additional Capital Costs, Pressurized Recycle Configuration.....	42
6. Control Overview .....	45
7. Controller Gain.....	46
8. Diesel-Generated Electricity Costs .....	50
9. Scale Inhibitors.....	66



## 1. INTRODUCTION

### 1.1 Significance and Objectives

As is this case with much of the Southwestern United States, Texas persistently faces water shortage issues across much of the state. As rapid population growth continues, the demand for water will continue to expand, exacerbating existing shortages.

In other parts of the world that have experienced similar shortages, desalination has successfully met the need in many cases. Several Middle Eastern nations such as Israel and Saudi Arabia obtain freshwater by desalination of brackish or sea water. Energy-intensive thermal desalination methods have given way in recent years to reverse osmosis (RO) technologies which offer fresh water at around half the energy cost [1].

In arid southern and western Texas, brackish ground water and oilfield produced water suitable for RO desalination are widely available and could potentially meet the region's water needs for the foreseeable future. The Permian Basin in Western Texas yields about 400 million gallons of saline water per day as a byproduct of petroleum production [2]. This is larger than the daily water usage of Houston, Texas.

Desalination of oilfield produced water is desirable for another reason. Disposal of produced water from oil and gas wells is a costly procedure for production companies. Water-to-oil production ratios generally increase as wells' production lives progress, exceeding 10:1 (by volume) in many cases [3]. This increase with its associated costs creates the bottleneck that prematurely ends the production life of many wells [4]. The water contains a number of contaminants, notably high salinity, hardness minerals, hydrocarbons, surfactants and other chemicals used in the production process, and sometimes heavy metals. Currently, common practice at onshore wells is to dispose of the brine by injecting it into disposal wells. Since the disposal wells are usually offsite, the production company incurs transportation costs in addition to injection costs. Clearly, reduction in the volume of this wastewater would benefit oil producers.

Previous research at the Global Petroleum Research Institute at Texas A&M University has explored and identified treatment options that are capable of recovering a high proportion of fresh water from oilfield brine. Technologies examined for hydrocarbon removal included centrifugation, flotation, adsorption, and ultrafiltration, while various nanofiltration and reverse osmosis membranes were considered for demineralizing and desalinizing the water. Organo-clay adsorbant was found to be the most effective method for de-oiling, while reverse osmosis membranes were chosen over nanofiltration membranes due to superior salt-rejection characteristics [5]. A small pilot unit was built and tested, and more recently a second, larger, trailer-mounted unit has been completed. However, some difficulties and questions remain concerning the technology. Three remaining tasks that are addressed in this project are:

- 1) Optimizing the process design for energy efficiency
- 2) Developing a control system to automate and simplify the unit's operation
- 3) Determining how to power the units when they are located in remote locations away from the power grid

The most obvious option for providing power in remote locations is portable, fossil fuel burning generators. However, high fuel and maintenance costs, as well as environmental concerns, have sparked interest in using renewable energy sources instead. Many of Texas' dry, oil-producing regions are fortunately blessed with high winds and/or particularly sunny weather, making economical solar and wind energy usage a realistic possibility with current wind turbine and photovoltaic technology. Far west Texas has some of the highest levels of solar insolation in the United States (see Appendix D). Coastal southern Texas, parts of western Texas, and the Texas Panhandle have class 3 or stronger winds on a scale of 1 (lowest) to 7 [6]. Class 3 winds (11.5-12.5 mph) are generally considered marginally suitable for electrical power generation, with class 4 (12.5-13.4 mph) or above preferred. As the cost of generation has dropped, many "wind farms" have been erected in Texas over the past 10 years. As of February 2006,

28 plants were operational, most of which are located in the western half of the state [7]. The rapid proliferation of these plants is indicative of the region's potential for meeting more and more of future power needs with wind. By powering desalination units with wind and/or solar energy, it is hoped that economically-viable freshwater could be made available in an environmentally-benign way.

## **1.2 Historical Perspective**

### **1.2.1 Reverse Osmosis**

The history of reverse osmosis begins with French scientist Abbe Nolet in 1748. That year, he observed solvent passing through a semipermeable membrane from a solution of lower concentration to one of higher concentration. Thus the principle of osmosis became known to the scientific world. Then, in 1877, Pfeffer measured the osmotic pressures of solutions of various compositions, and noted that osmotic pressure increases with temperature, and that the ratio of osmotic pressure and temperature remained constant in his experiments. Van't Hoff, a Dutchman, took the next step and incorporated those observations into a well-known equation now bearing his name, which states that osmotic pressure is equal to the product of solute concentration, temperature, and the universal gas constant,  $\Pi = cRT$ . Identification of this relationship, valid for dilute solutions, helped earn van't Hoff the 1901 Nobel Prize for Chemistry.

Only in the 1950's did the scientific community begin seriously studying reverse osmosis as a method of water treatment. In 1953, the U.S. government's Office of Saline Water began funding reverse osmosis research. The University of Florida's Reid and Breton began investigating cellulose acetate as a potential membrane material. Then in 1960, Loeb and Sourirajan made a great stride in cellulose acetate membrane development, creating a film with about 500 times greater permeability than the original. At General Atomic, Westmoreland and Bray developed the now-dominant spiral-wound membrane configuration for R.O. membranes in 1966. As the technology continued to become more established and economical, applications arose for it in military, municipal, and commercial settings during the late 1960's and early 70's [8]. The 80's and 90's have seen the emergence of polyamide as the preferred material for reverse

osmosis membrane construction. Also, reverse osmosis surpassed thermal methods (i.e. distillation) as the world's dominant water desalting method.

### **1.2.2 Solar Energy**

The origin of photovoltaics can be traced to French physicist Alexandre Becquerel's 1839 discovery of the photoelectric effect – the conversion of light to electricity. Nearly 40 years later, in 1877, the first selenium solar cell was constructed. In the early 20<sup>th</sup> century, Albert Einstein developed the theory behind the effect, and was awarded the 1921 Nobel Prize for the accomplishment. Bell Laboratories in New Jersey made a breakthrough in 1954 when they created cells with 4.5% efficiency, improving it to 6% within a few months. Their effort was an offshoot of America's space program research. Consequently, the cells' original application was as a power source for satellite electronics. In 1963, Sharp Corporation created the first usable module of silicon cells, the arrangement that most modern PV devices utilize [9].

Meanwhile, the use of solar energy for desalination began with solar distillation. While people have distilled seawater for hundreds of years in order to obtain salt, distillation for the purpose of purifying water was first carried out on a large scale in Chile in 1872. There, a solar distillation apparatus provided drinking water for a mining community. While never enjoying widespread application, a resurgence in interest in the concept emerged among scientific community in the 1950's has resulted in improvement of the technology. A modern, multistage solar distillery is reported to produce about three times as much water as traditional designs [10].

### **1.2.3 Wind Power**

Wind energy has been used by humans far back in history, first to propel sea vessels, then later, beginning about 4000 years ago, to operate windmills. Traditionally, grain and spices have been ground by windmills, and timber has long been cut in wind-powered sawmills [11]. Then, in 1888, Charles Brush of Cleveland, Ohio built the first large windmill for electricity generation. Shortly thereafter the term "wind turbine" came into use in describing wind-powered electrical generators. Early in the 20<sup>th</sup> century the

Jacobs turbine, an early 3-blade turbine resembling modern designs, grew in popularity in rural America. It was often incorporated into home power systems with battery storage. However, with the expansion of power grid networks under the Rural Electrification Administration during the 1930's, the wind-generated electricity industry in the United States dwindled then virtually disappeared. Europe also developed and utilized wind turbines during the late 1800's and early 1900's. In Denmark, Poul La Cour built over 100 mid-sized turbines, with 20-35 kW nominal capacities, between 1891 and 1918. As in the U.S., wind power in Europe experienced a lull in popularity during the middle of the 20th century. With the emergence of environmentalism and concern over fossil fuel use during the 1960's, wind power began to attract attention again. Then, the oil embargo of 1973 sparked an energy crisis, and wind and other renewable energy sources surged in popularity, benefiting from government research programs, tax incentives, and other financial support. California, with its many excellent sites for wind farms, as well as favorable state tax incentives, became the focal point of the American wind industry. There, many wind farms were erected in a short period of time. However, the California wind industry had shrunk significantly by the next decade, crippled by the unreliability of hastily-engineered, untested turbines, as well by the removal of some of the tax incentives. Most U.S. turbine manufacturers went out of business, and since that time the wind industry has seen the lion's share of its growth in Europe [12].

## 2. THEORY AND LITERATURE REVIEW

### 2.1 Membrane Basics

The American Heritage Dictionary [13] defines a membrane as “A thin sheet of natural or synthetic material that is permeable to substances in solution.” Membranes are ubiquitous in the world, found in natural systems such as living cells, as well as in industrial, commercial, and residential applications. Membranes are sometimes used in gas separations but are especially prolific in liquid applications. In the most conventional arrangement, dead-end filtration, a fluid is passed through a barrier, leaving behind one or more components. Some applications are better suited to cross flow arrangements, as illustrated in Figure 1. With a substantial portion of the flow occurring tangentially to the membrane surface, this arrangement reduces buildup of plugging materials at the membrane surface since most of the material is swept downstream.

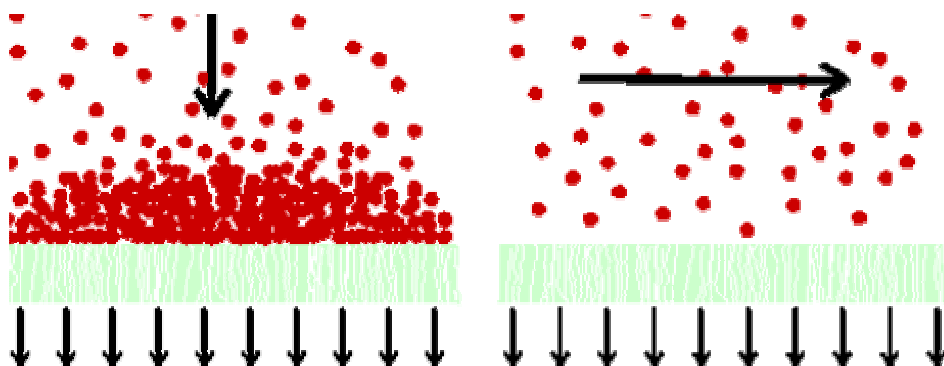


**Figure 1. Dead-End and Cross Flow Filtration [14]**

The application of pressure-driven cross-flow membrane processes to water treatment has become increasingly common over the last 20 years, as the quality of the technology has shown improvement and costs have shrunk. Reverse osmosis, nanofiltration, ultrafiltration, and microfiltration constitute the major categories of pressure-driven membranes, categorized according to pore size. Figure 2 illustrates the capabilities of each.

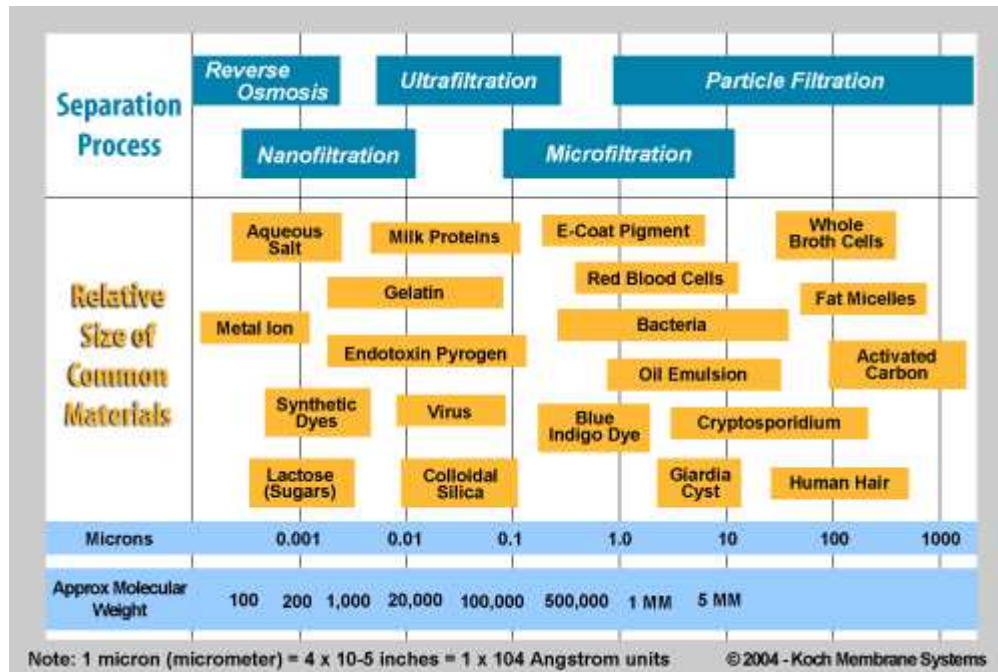


**Figure 2. Membrane Separations Spectrum [15]**

Manufacturers have utilized several designs for cross flow membrane devices. Tubular, plate-and-frame, spiral-wound and hollow-fiber configurations are available, the latter two being most common [16]. Spiral wound membranes are made by attaching several membrane sheets to a cylindrical core, then winding the membranes into a compact cylinder (see Figure 3). Hollow fiber designs feature a large number of thin, flexible membrane tubes glued together at one end. While hollow fiber membranes have greater surface area per unit volume, spiral-wound designs dominate the reverse-osmosis industry due to a lower propensity for fouling.

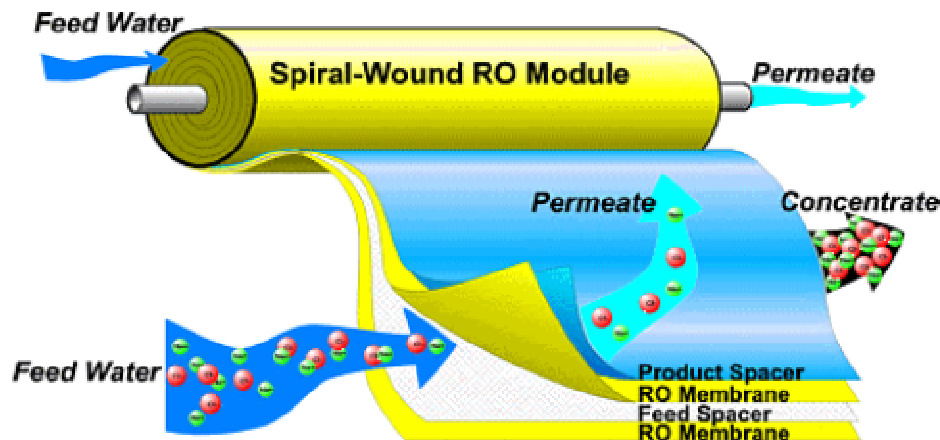


**Figure 3. Spiral-Wound Membrane [17]**

Reverse osmosis and nanofiltration membranes are usually made of synthetic organic polymers. Until the 1990's, cellulose-derived membranes such as cellulose acetate and cellulose triacetate were the most common variety. They have the advantage of withstanding chlorine-treated waters, but are susceptible to damage from extreme pH, high temperature, and biological degradation [16]. Presently, however, other membrane material types have far-surpassed cellulosic in popularity. Hydrophilic polymers, especially polyamides, are commonly used in desalination membrane manufacture due to their greater tolerance for acidic/basic conditions and wider temperature operating range. Unfortunately, they are easily damaged by even minute concentrations of oxidants (most manufacturers recommend <0.1 ppm chlorine).

## 2.2 Measures of Membrane Performance

The following two equations describe the diffusion of water and a solute, respectively, across a semipermeable membrane [16].

$$F_w = A(P_{tm} - \pi_{tm}) \quad (1)$$

Where:

$F_w$  = water flux (g/(cm<sup>2</sup>·s))

$A$  = water permeability coefficient (g/(cm<sup>2</sup>·s·atm))



$P_{tm}$  = pressure differential across the membrane (atm)

$\pi_{tm}$  = osmotic pressure differential (atm)

$$F_s = B(\Delta C_s) \quad (2)$$

Where:

$F_s$  = solute flux (g/(cm<sup>2</sup>·s))

$B$  = solute permeability constant (cm/s)

$\Delta C_s$  = Solute concentration difference across the membrane (g/cm<sup>3</sup>)

From these simple equations, it is evident that water flux is proportional to applied pressure, while solute flux is not; therefore one basic fact of reverse osmosis separations is that higher operational pressures lead to lower salinity in the product water.

The constants  $A$  and  $B$  in the above equations are membrane specific;  $B$  is also solute specific. Boundary layer effects as well as a concentration gradient along the length of the membrane complicate the use of the above equations in predicting membrane performance. Because membrane performance is difficult to model from first principles, many membrane manufacturers provide design software to allow engineers to predict the performance of their products under various operating conditions. These programs are based on empirical models developed from performance data acquired through extensive membrane testing.

Some basic terminology used in describing reverse osmosis performance and operating conditions follows:

*Recovery:*

$$Y = \frac{Q_P}{Q_F} \times 100 \quad (3)$$

Where:

$Y$  = Recovery (%)

$Q_P$  = Permeate Volumetric Flow Rate (l<sup>3</sup>/min)

$Q_F$  = Feed Volumetric Flow Rate (l<sup>3</sup>/min)

*Solute Rejection:*

$$R = \frac{C_f - C_p}{C_f} \times 100 \quad (4)$$

Where:

$R$  = Solute rejection / removal (%)

$C_p$  = Concentration of solute in permeate stream (mg/l)

$C_f$  = Concentration of solute in feed stream (mg/l)

*Transmembrane pressure:*

$$TMP = \frac{P_f + P_c}{2} - P_p \quad (5)$$

Where:

$TMP$  = Transmembrane pressure (psi)

$P_f$  = Feed pressure (psi)

$P_c$  = Concentrate pressure (psi)

$P_p$  = Permeate pressure (psi)

Another concept that has a notable effect on reverse osmosis membrane performance is that of concentration polarization, a phenomenon in which solute concentration near the membrane surface exceeds the concentration in the bulk liquid. Some degree of concentration polarization occurs in all reverse osmosis systems. As solvent passes through the membrane, solute builds up at the membrane surface, establishing a concentration gradient at the membrane surface which provides a driving force for diffusion away from the surface. Figure 4 illustrates the situation. A high degree of turbulent mixing can minimize the width and intensity of this boundary layer, reducing concentration polarization. In terms of RO operating parameters, reducing recovery and/or increasing feed flow rate reduces concentration polarization effects.

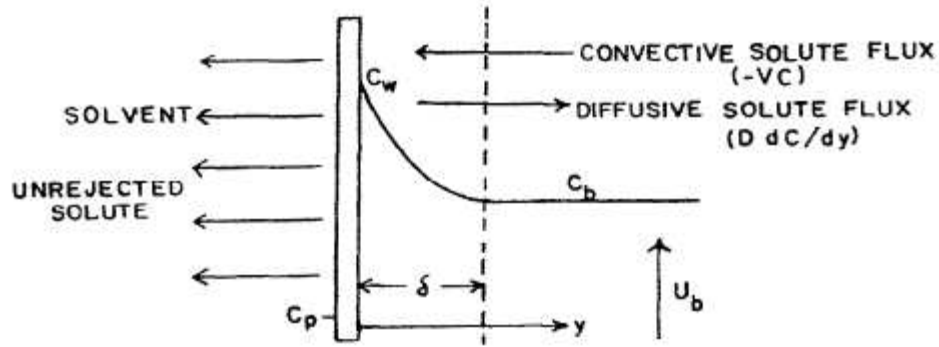


**Figure 4. Concentration Polarization [18]**

Quantitatively, the phenomena can be described by the following equation

$$VC_p + VC + D \frac{dc}{dy} = 0 \quad (6)$$

Where:

$V$  = volumetric flux rate of solvent through the membrane ( $\text{cm}^3/(\text{s}\cdot\text{cm}^2)$ )

$C$  = concentration of solute ( $\text{g}/\text{cm}^3$ )

$C_p$  = concentration of solute in permeate ( $\text{g}/\text{cm}^3$ )

$D$  = diffusion coefficient of solute in solvent ( $\text{cm}^2/\text{s}$ )

With boundary conditions:

$y = 0$  (surface),  $C = C_{wall}$

$y = \delta$  (edge of boundary layer),  $C = C_{bulk}$

Concentration polarization may then be defined as  $C_{wall}/C_{bulk}$ . In addition to promoting precipitation and, hence, membrane scaling, two other undesirable effects occur. Solute rejection is reduced because the high concentration of solute at the surface causes more to diffuse across the membrane into the product stream. Thirdly, solute flux across the membrane declines due to the higher osmotic pressure in the concentrated boundary layer that must be overcome to achieve the separation [18].

### 2.3 Membrane Fouling

Over time, membrane performance inevitably declines as indicated by higher pressure drop across the membrane, and/or reduced quality and quantity of product water. All spiral-wound units experience some reduction in performance during the first few hours of operation due to compaction of the membrane surface. Compaction reduces the permeability of the membrane, resulting in decreased product flux. It is a well-understood phenomenon, and is always accounted for by competent designers. However, as service lifetime progresses, membranes almost always experience reduced performance due to fouling – the accumulation of undesirable materials on the membrane surface. In addition to degrading performance, severe fouling can cut short the useful life of a membrane. The many causes for fouling can be categorized as being physical, chemical, or biological in nature.

Physical fouling consists of membrane performance degradation due to the buildup of solid materials such as colloids, humic substances, oils, greases, rust, and other materials that can accumulate at the membrane surfaces, but that do not undergo chemical changes while in the membrane system. They may lodge in pores in the membrane surface, reducing membrane permeability. Larger particles may simply build up as a cake at the membrane surface, creating additional resistance to fluid flow as the cake thickens [19]. For cross flow membranes it is frequently recommended that particles more than one fifth of the size of the membrane's water channel are to be avoided due to their tendency to become lodged in and obstruct the channel. Two feed water parameters commonly used to predict physical fouling are the Silt Density Index (SDI) and turbidity. Typically, RO membrane manufacturers strongly recommend that feed water has  $SDI < 5$  and/or turbidity  $< 1$  ntu [16].

The second form of fouling is chemical fouling, namely scaling. Scaling is the buildup of precipitated solids on surfaces in contact with water. In RO and nanofiltration systems, mineral salts can precipitate out of solution when they exceed solubility limits as they are concentrated by the desalination process. These solids then can accumulate at the membrane surface, obstructing flow and perhaps physically damaging the membrane. The most common agents responsible for membrane scaling are calcium carbonate ( $CaCO_3$ ), sulfate salts ( $CaSO_4$ ,  $BaSO_4$ ,  $SrSO_4$ ), and silica ( $SiO_2$ )

[16]. This form of fouling is highly preventable if feedwater composition is known, since the solubility limits of the responsible compounds are well documented. Plant operating conditions such as feedwater pH and recovery can be selected such that precipitation does not occur, and anti-scalant chemicals are also commonly used to allow for greater fresh water recovery while still avoiding scaling [19].

Perhaps the most challenging form of fouling is that caused by biological contaminants. Unlike other types of fouling, biofouling can not necessarily be controlled by reducing foulant concentration in the feed water. Biofouling can be destructive to membranes in two ways: 1) mechanically obstructing the flow of water across the membrane (in much the same way as physical fouling), and 2) chemically degrading the membrane itself. Biofouling generally begins with the growth of biofilm at the membrane surface. Biofilm is a layer of microorganisms, usually embedded in a protective layer of extracellular polysaccharides (EPS). As the film grows and begins to noticeably affect membrane performance, it is termed “biofouling.” The bacteria present in biofilm feed on organic compounds, so feedwater Assimilable Organic Carbon (AOC) is a key parameter for biofilm growth. Approaches to control of biofouling include reducing AOC and killing the microorganisms with biocides [20].

A more extensive overview of scaling and biofouling prevention and treatment methods is included in the Appendix.

## **2.4 Literature Survey: Treatment of Produced Water**

Treatments for produced water have been the subject of numerous published studies. The following is a sampling of recent efforts. In 2002, Funston et. al. [21] conducted a pilot study of a treatment for produced water consisting of several unit operations. The treatment consisted of coconut shell filtration, cooling, a trickling filter, ion exchange, and reverse osmosis. Ammonia, boron, organics, oil and grease, silica, hardness, and salinity were all targeted for removal in this extensive treatment scenario. Levelized treatment cost of the water was estimated at \$0.12 per barrel (industrial-use quality) to \$0.50 per barrel (drinking-water quality) for the process.

Prior to Funston's study, a group of engineers at Kvaerner examined treatments for removing dissolved contaminants, specifically for the offshore environment [4]. They concluded that no single treatment was adequate to remove all pollutants: multiple technologies were needed. For heavy metal removal, they felt that ion exchange was the best available technology. Air stripping, activated carbon, and biological treatment were all necessary to remove organic foulants. The authors also noted the potential of membrane processes to de-toxify the water, although at the time of the study, membrane technology in general and energy efficiency in particular was not nearly as good as it is at present.

Bourcier et al. [22] developed a treatment process for produced water at a Polish coal mine. The four-step process focuses on preventing mineral scaling from occurring at the surface of the reverse osmosis membrane. In the first step, the water is coarsely filtered to remove suspended solids particles. Next, sodium carbonate is added to the water, which causes precipitation of sulfates, oxides, and carbonates from the solution. In the third step, microfiltration removes the precipitated solids, leaving the water with lower levels of potential scaling minerals. Hydrochloric acid then is added to lower the pH, since most minerals precipitate more readily at higher pH. Then, salts are removed by reverse osmosis, leaving concentrated brine with about 73,000 ppm dissolved solids content as the waste stream. The researchers utilized geochemical modeling software to consider the potential for scaling and develop the proper dosing of  $\text{NaCO}_3$  and  $\text{HCl}$ . The findings made with the software were verified by laboratory tests, which showed "fairly good" agreement. The disagreement was due to Barium and Magnesium levels in the post- $\text{NaCO}_3$ -addition water being higher in lab tests than in model predictions. The author emphasized that while the process may be applicable to other saline waters, the chemical dosages are unique to the chemistry of the water being treated.

## **2.5 Renewable Energy and Applications to Desalination Processes**

Both photovoltaics and wind turbines have been used to power reverse osmosis processes in studies conducted by several investigators. Following is an overview of the technologies, followed by a literature survey of their application to desalination.

### 2.5.1 Photovoltaics

Photovoltaic cells are semiconductor devices, usually consisting of silicon doped with impurities. Light striking the cells induces electron flow and, hence, current. Each individual cell produces about 0.5 volts. A number of cells are wired together in series to produce a higher voltage, usually around 17-18 volts, a practical level for charging 12-volt batteries. The linked cells, called “modules” are enclosed in a weatherproof casing with a transparent (usually tempered glass) cover and a frame of aluminum or other rigid material. About 10-12% of the solar energy striking a modern, single or polycrystalline PV panel is converted to electricity, compared with about 6% efficiency in Bell Labs’ original unit. Less-costly amorphous / thin film types offer 5-7% efficiency. While insufficient data exists to authoritatively predict the functional lifetime of PV panels, most manufacturers warranty their products for 10-20 years, and it is thought that lifetimes will be measured in decades. Some performance deterioration occurs: about 0.5 to 1% per year for single- and polycrystalline units, and a substantial initial drop followed by stabilization for amorphous silicon.

### 2.5.2 Wind Power

Wind turbines are machines which harness the kinetic energy of the wind to do useful work such as pumping water or generating electricity. A wind turbine absorbs power according to the following equation:

$$P = 0.5\rho AC_p V^3 \quad (7)$$

Where:

$P$  = power generated by the wind turbine (W)

$\rho$  = air density ( $\text{kg/m}^3$ )

$V$  = wind speed (m/s)

$A$  = rotor swept area ( $\text{m}^2$ )

$C_p$  = power coefficient

If the power coefficient is removed from the above equation, the remaining expression gives the power contained in the wind's motion. The power coefficient is the fraction of that power that can be extracted by a given turbine. According to Betz's limit, the theoretical maximum value for the coefficient is 59%. More recently, Gorlov [23] showed that the limit for a propeller-type rotor is about 30%. Actual values for turbine-type propellers are typically 10-20%, and depend on aerodynamic properties of the turbine as well as wind conditions. Since in the above equation the power generated is proportional to the cube of the wind velocity, a seemingly minor change in wind speed can have a great effect on power production. Thus an accurate knowledge of a site's wind characteristics is critical to determining the economic feasibility of wind power in that location. It can also be observed from the equation that power is proportional to wind density, so colder regions, with correspondingly denser air, are also favorable for wind power generation. For example, dry air near sea level at 80°F would have a density of about 1.17 kg/m<sup>3</sup> while air at 40°F is 8% denser, 1.27 kg/m<sup>3</sup>.

### 2.5.3 Literature Survey

Many scientists have utilized wind power to desalinate water in remote locations. Most attempts have taken the approach of utilizing wind power to generate electricity to drive the pumps for the reverse osmosis process, while some others have attempted to power the pumping process mechanically, without any intermediate electricity generation.

One project which falls into the later category was that of Liu et al [24] at the University of Hawaii. The system used a high-torque, multi-vaned windmill to directly drive a pump to pressurize brackish water. The water enters a tank that contains a bladder of pressurized air, increasing pressure as more water enters and compresses the air. Once the pressure reached a preset value, the control system opened a solenoid valve, releasing pressurized water to the reverse osmosis membrane. At some lower limit of feed pressure, the valve is closed and pressure allowed to build up again. In practice, three parallel valves were employed to allow for more operational flexibility, since winds and hence pumping rates vary drastically.



Field experiments showed that the apparatus could produce 2.7 l/minute (~4000 liters/day) with an average wind speed of about 5m/s, and feed water of 3000 mg/l Total Dissolved Solids (TDS).

Habali and Saleh [25] examined a more conventional process, involving electricity generation to drive pumps. They conducted an economic comparison of wind-powered versus diesel powered RO desalination in a desert region of Jordan. Field tests were not conducted; costs for the wind and diesel generators were calculated from literature and manufacturer's data. Desalination energy requirements were based on brackish well water as feed, which requires much less energy than seawater. The region studied had a 4.4m/s average annual wind speed, and 14kW and 20kW-rated wind turbine generators were compared with similar sized diesel generators. The wind-powered process was found to be more economical.

Kiranoudis [1] also explored the use of wind power for desalination. He considered wind power as a supplement to power from a grid, not as a stand-alone source. His studies were of larger scale turbines, of a diameters of 28 and 42 meters, with nominal power outputs of 59 kW (at 7.2m/s wind) and 170kW (at 8.2m/s) respectively. He concluded that, with average annual wind speeds of 5m/s or greater, unit costs of product water can be reduced by up to 20% by utilizing wind power. He also stated that, below roughly 5 m/s average wind speed, exploiting wind energy would not be economically beneficial.

Another scientist to study wind-powered desalination is L. Garcia-Rodriguez. Like Kiranoudis, she focused on larger –scale wind turbines; specifically, three with diameters of 43, 44, and 48 meters. She determined the primary factors influencing the levelized cost (LC) of desalinating water to be plant capacity, climatic conditions, and the energy requirement of the plant, which energy requirement depended on several factors such as feed water salinity.

Garcia-Rodriguez [26] identified climatic conditions of importance to wind turbine electricity generation as average annual wind speed (VM) and the Weibull shape parameter (k). The shape parameter describes the distribution of wind speeds over time for a given location. Naturally, more power is generated at higher wind speeds. The relationship between shape parameter and power generation is less obvious. According

to Garcia-Rodriguez, if wind speed is greater than 8m/s, levelized cost slightly decreases with  $k$ , but if wind speed is less than 7m/s, LC increases with  $k$  (7). From this it can be inferred that above 8m/s power generated increases with  $k$ , and below 7m/s power generated decreases with  $k$ . In any case, the effect of  $k$  is small compared to the effect of average wind velocity. Kiranoudis states that, for most regions,  $k$  varies between 1.8 and 2.2, and within that range its effect is “practically negligible.”

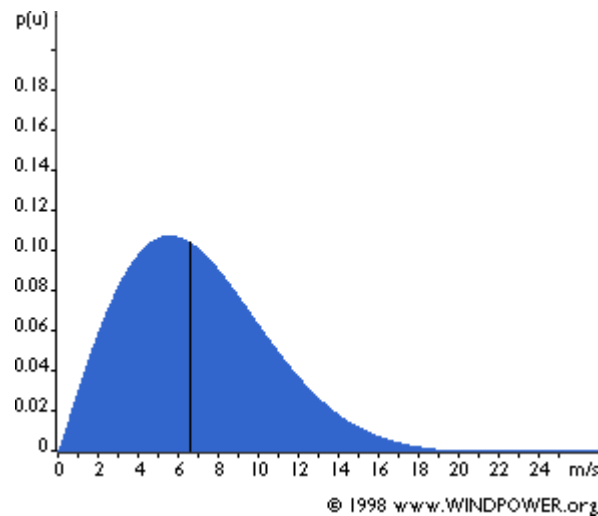


**Figure 5. Weibull Distribution**

Figure 5 shows a Weibull distribution with a shape parameter of 2, also known as the Rayleigh distribution. The mean wind speed is 7m/s and the median is 6.6m/s (21).

In another case, Kershman et al [27] simulated a small-scale desalination plant powered by an electric grid supplemented by wind generated and photovoltaic electricity. The simulated system was designed to produce two streams of up to 150m<sup>3</sup> water per day from seawater, requiring 70kW of electricity, AC. The PV field had a 50kW peak capacity, and the wind-powered generator was a nominal 200kW unit. Climatic data were recorded at a small Mediterranean island in Tunisia, having an average annual wind speed of 4.4m/s. Solar irradiation statistics for the area were compiled as well. The simulation indicated that the solar panels were capable of providing about 11% of the annual operating electricity, while the wind generated power

would meet 57% of the need. During peak times, combined power from wind and PV would exceed demand, and the excess would be fed back into the grid. The quantity fed back amounts to 2% of the annual energy demand.

Kershman also included an economic analysis as part of the study. Key results include levelized energy costs of 0.035 \$/kWh for grid power, 0.12 for combined grid plus PV power, 0.105 for grid plus wind power, and 0.195 for all three combined. Levelized water costs show less dramatic price increases for the renewable sources; grid only results in \$1.266/m<sup>3</sup> compared with 1.757, 1.664, and 2.167 for grid plus PV, grid plus wind power, and grid plus PV plus wind power, respectively [28].

Weiner et al [29] built a functioning RO desalination plant powered entirely without relying on a power grid. His system incorporated a PV array and a wind turbine, and used a deep-cycle battery bank to store excess power and to provide for more continuous operation. The RO unit was smaller than those previously discussed. It desalinated brackish water, producing 3 m<sup>3</sup> per day of fresh water. The PV modules served as the primary power providers in this system, with a peak output of 3500W, while the 600W wind turbine served to “top off” the battery bank, as the author explains. A 2200W motor driving a centrifugal pump consumed most of the energy. The system was operated for about 4 hours per day, which was less than had been planned because the RO unit consumed about 30% more energy than the design specified. Weiner stated in his concluding remarks that the appropriate ratio of power required to peak power generated is of the order of 30-50%.

Mohamed and Papadakis [30] designed a stand-alone, solar and wind powered desalination unit for a remote Greek village. The unit was designed to provide 0.5 m<sup>3</sup>/hr of fresh water from 40,000 ppm-TDS seawater feed, using three 4”x 40” spiral wound membranes. A key element in the design was the incorporation of a pressure-exchanger device, uncommon for such a small system. The authors claimed that the unit reduced the energy requirement of the high-pressure pump by 48% from 12 kWh/m<sup>3</sup> to 6.3, reducing the size of the needed pump as well as the energy generation system. Power storage was provided by a bank of lead-acid batteries, sized to provide 2 days of storage. Before deciding on a hybrid system of 40% PV and 60% wind, the authors conducted an

economic evaluation which considered all-PV, all wind, and several combinations of the two. The selected design had an estimated cost of \$6.47/m<sup>3</sup> of fresh water [28].

Thomson and Infield [31] offered a unique approach to desalinating water with PV power. They proposed a design for a seawater reverse osmosis system that did not include batteries. The design called for a progressing cavity Moineau pump to deliver medium-pressure water from a beach well. A novel energy recovery device would increase the pressure to operational levels. The device, called a Clark pump, mechanically fixes the recovery at 10%, but an additional high pressure pump was included in the design to allow higher recoveries. A custom control algorithm would distribute power from the PV panels to the two pumps in such a way as to optimize fresh water production depending on solar intensity. A model of the entire system was completed in Matlab / Simulink, with the most critical component performances verified by lab trials. The design's 2.4 kW PV array was predicted to deliver over 3m<sup>3</sup>/day of fresh water. Economic analysis showed a cost of \$3.27/m<sup>3</sup> for product water, although it should be noted that the analysis did not include equipment shipping or installation costs.

The same scientists considered wind turbines to power an otherwise similar process in another paper [32].

## 2.6 Dynamic Simulation and Control System Design

Rahbar [33] explains some of the benefits of using dynamic simulators in process design, specifically for desalination processes. He asserts that modeling and simulation helps “test and validate” a process in a cost-effective manner before committing to the expense of building a pilot unit or plant. Dynamic simulators are particularly useful in studying plant controllability. He proceeds to describe the basic character and structure of Speedup (the forerunner of Aspen Dynamics). It is a Differential and Algebraic Equation (DAE) – based simulator. The user interfaces with the *executive* portion of the program, which creates a database containing the process/problem description. This information is translated and passed to the *run-time* program, which solves the problem with any of a number of available numerical methods. The *run-time* also contains

routines to carry out physical property calculations. With the *run-time*'s output, the user can create graphs, charts, tables etc. to display simulation output using the *results presentation tools*.

William Luyben has done extensive research on controlling processes that contain recycle loops, and is an expert in the use of process simulators. As he wrote in a 1993 publication [34], “processes with recycle streams are quite common but their dynamics are poorly understood.” Some of his writings aim to guide engineers in designing such processes.

Luyben has discussed the use of Aspen Dynamics in converging process flow sheets with recycle streams [35]. Recycles (or “tear streams”) in process simulators require the simultaneous solution of many nonlinear algebraic equations, a mathematically difficult task for which there is no algorithm that will work every time. Even when the user provides a starting value for a recycle stream that is very close to the actual solution, steady-state simulators still sometimes fail to find the solution. Dynamic simulators can aid the engineer in reaching a solution. Luyben explains the procedure for converting an Aspen Plus simulation to Aspen Dynamics. For example, the size of tanks and other equipment that has holdup must be specified in Dynamics, while this step is unnecessary in a steady state simulator. After explaining Dynamics' default control setup, Luyben gives several rules for creating an effective control structure. Among these are:

- 1) placing flow controllers in all liquid recycle loops and
- 2) controlling all liquid levels, and pressures in gas systems

He also recommends initially setting the tuning parameters of all flow controllers to an integral time of 0.3 minutes and a gain of  $\frac{1}{2}$ .

Practical guidelines for controlling positive displacement pumps are given in abundance by Driedger [36]. Positive displacement pumps exhibit a performance curve much different from that of the centrifugal pump; a plot of pressure versus flow gives a nearly-vertical line, indicating that they operate at constant flow with the pressure rising to virtually whatever value is necessary to attain that flow. Unlike centrifugal pumps, discharge throttling is not an option for flow control, and suction throttling is likewise futile and likely to cause cavitation. Available flow control methods are recycle control

(recycling a portion of the discharge back to the feed tank) or motor speed control. Two cautions given for the application of recycle control are to avoid recycling directly back to the suction pipe, since this does not allow air bubbles to escape, and to select the recycle valve carefully so as to avoid cavitation if the pressure drop is large. Speed control is effective and simple since flow rate is proportional to pump speed. Although theory suggests that any point on the system curve can be reached using this control method, this is not necessarily true because most variable-speed drives have a lower speed limit which restricts system turndown. Also, rapid changes in pump speed are not possible due to the inertia of the fluid and pumping machinery. Therefore, the system should not be expected to react quickly to, for example, the rapid closure of an upstream valve. In such a situation, overpressure could easily result.

Most positive displacement pumps are used in high-pressure service. Flow is in a pulsating manner, so many applications benefit from the addition of a hydraulic pulsation dampener. If sensitive flow or pressure control is required, larger pulsation dampeners will enhance performance, and pressure gauges can be fitted with “snubbers” to diminish pulsations further. Finally, Driedger emphasizes that pressure relief near the pump discharge, and possibly also near the inlet, is an important precaution against overpressure, which is the greatest operational hazard for positive displacement pumps.

### 3. PROCESS DESCRIPTION AND DESIGN ALTERNATIVES

#### 3.1 Existing Design

Personnel in the Separations Sciences group at the Food Protein Research and Development Center of the Texas Engineering Experiment Station have assembled a pilot unit that is currently being used for performance studies and technology demonstrations. This unit is the “Existing” or “Original” design referred to in this document. In the unit, the raw water is pumped through a wire strainer to remove any large particulate matter, then proceeds through a cartridge filtration step consisting of a 5- and/or 20-micron filter. To remove the remaining dissolved or emulsified hydrocarbons, the water then passes through a vessel of organo-clay adsorbant, at a rate that allows a residence time of 5 minutes or more to achieve the desired oil removal. Under consideration is an intermediate pretreatment step of microfiltration or ultrafiltration. The de-oiled water then passes through a high pressure, positive displacement pump to raise the pressure to reverse osmosis operating levels of 600 – 1200 psi. The reverse osmosis membrane splits flow into two streams, concentrate and permeate. Concentrate is the larger stream, typically 80-90% of process flow, and can be recycled back to the feed tank. The permeate, or fresh water, exits the process while the concentrate continues to be recycled until the salt concentration in the feed tank reaches an upper operating limit. The unit’s operation is summarized in Figure 6, a simplified flow diagram.

If a modest process yield of 10-20% fresh water is acceptable, recycling of concentrate is unnecessary. However, to achieve higher yields as would most probably be desired by a commercial/industrial user, recycle is required. In the existing design, no provision is made to recover the substantial amount of mechanical energy that is lost when concentrate pressure drops nearly 600 – 1200 psi when recycled to an atmospheric feed tank. This is a major source of inefficiency in the process and a flaw which the following proposed alternatives aim to overcome.

Also, the existing design lacks any automation. All valves are hand operated, and no transmitters or logic controllers are utilized.

## 3.2 Alternative Designs

### 3.2.1 Recycle to Pressure Vessel

The first alternative design attempts to retain the basic structure of the existing design. As can be seen from Figure 6, the pretreatment section remains the same. After passing through a high pressure pump, the water passes through a large, high-pressure tank en route to the reverse osmosis membrane, where it mixes with recycled concentrate from the membrane. Similar to the original configuration, the process continues until the salinity in the high-pressure tank becomes too high for economical desalination performance.

Several objectives must be met by the control system:

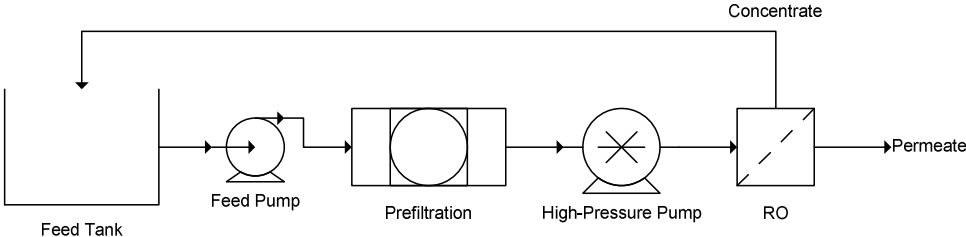
- 1) The flow rate must be controlled such that the 5-minute minimum residence time through the adsorbent media is maintained.
- 2) Flow rate to the membrane must be sufficiently high to prevent substantial concentration polarization from occurring at the membrane surface.
- 3) Pressure in the high-pressure tank must be maintained within operating limits.

The pressure is directly related to the level in the tank, since a pocket of compressed gas (nitrogen or air) will be present at the top of the tank, promoting a relatively stable pressure in the tank. Level change is proportional to the net accumulation in the tank, which is the difference between flow in through the high pressure pump and flow of permeate out of the system. Since permeation rate (flow exiting the system) decreases as the batch proceeds and feed salinity increases, the control system may need to reduce flow through the high-pressure pump in order to keep pressure from rising too high. This is compatible with control objective 1, since reducing the pumping rate will increase the residence time so there would be no threat of it falling below the 5-minute minimum.

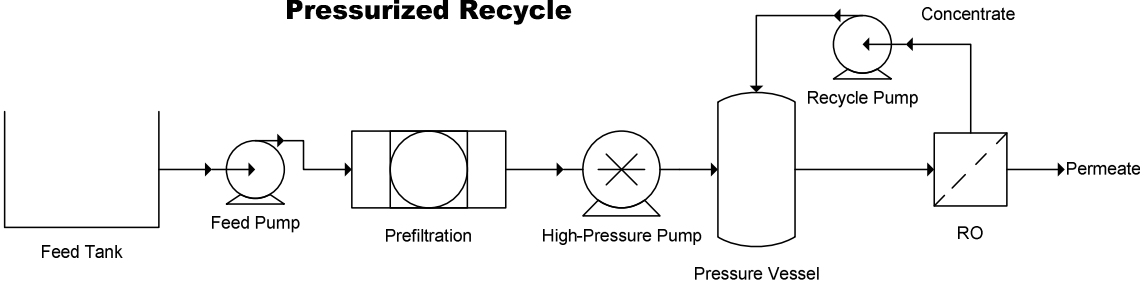
To achieve control objective 2, a control valve can be employed to maintain flow at a set point, with a centrifugal recirculation pump operating a constant speed providing the driving force for fluid flow. More details of the control system are given in Section 4.



**Existing Configuration**



**Modified Configuration – Pressurized Recycle**



**Modified Configuration – Membranes in Series**

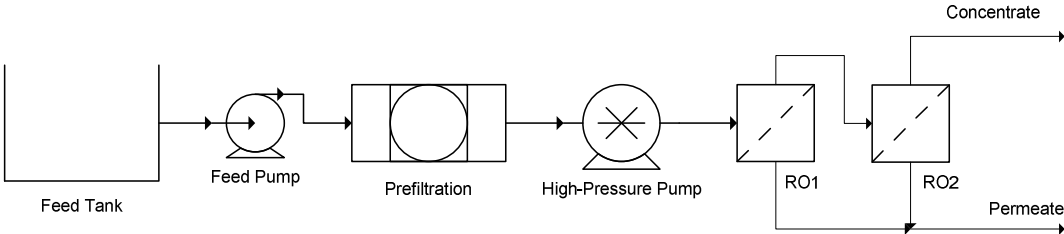


**Figure 6. Possible Process Configurations**

### **3.2.2 Multiple Membranes in Series**

This configuration would require only a slight modification of the existing setup. Instead of utilizing a single membrane, two or more would be arranged in series, such that the concentrate from the first would become the feed for the second, and so on. Such an arrangement would provide a larger recovery without any additional energy input, and only a small additional capital investment (the cost of additional membranes plus piping). The process control / automation strategy would be virtually identical to one for the existing process. It has the disadvantage of reduced flexibility since the process cannot be stopped at any arbitrary recovery level – each pass through the series of membranes would represent a large “step” in recovery. If desalination can only proceed to a certain recovery (to prevent oversaturation of a scaling mineral, for instance) then this design may not allow for a close approach to the desired endpoint.

## **4. COMPUTER SIMULATION AND CONTROL SYSTEM DESIGN**

Most reverse osmosis membrane manufacturers provide simulation software to predict the performance of their products under various operation conditions including feed temperature, pressure, and salinity. However, these software products predict steady state operating conditions for a continuous process, and are not capable of simulating a batch process. Because the processes of interest are batch, it was necessary to use a dynamic simulator. Since Aspen Dynamics is a highly reputable dynamic simulator and is available to Texas A&M University students, it was chosen for use in this project.

### **4.1 Methodology**

#### **4.1.1 Flowsheet Creation**

Aspen Dynamics requires that the user first create the simulation flow sheet in Aspen Plus, a steady-state simulator. After running the steady-state simulation without errors, it can be exported to Aspen Dynamics. However, the pressurized recycle configuration never reaches a steady state. The salt content of the water in the pressurized tank continually increases over the duration of the batch since concentrate is recycled into it. To overcome this difficulty, it was necessary to create the Aspen Plus simulation with fresh water feed, eliminating the changing composition. With fresh water feed, process conditions do not change with time so the process operates at steady state. After running in Aspen Plus, the simulation was exported into Aspen Dynamics, where feed composition could be changed to the desired salinity.

#### **4.1.2 Incorporating RO Membrane Model**

Aspen lacks a “built-in” reverse osmosis unit operation, presenting another challenge in creating the simulation. However, Aspen’s Custom Modeler software allows the user to program custom unit operations in Fortran, which can then be used in steady-state or dynamic simulations. An empirical model of membrane performance developed by A&M researchers from RO operating data was to be the core of the custom

model. After spending considerable time in creating a custom model of a reverse osmosis membrane from scratch, a functional model was not forthcoming. At that point, further study of Aspen Dynamics and Custom Modeler help files and examples yielded the discovery of another method that would produce results of sufficiently high accuracy.

The alternative method uses Aspen’s built-in, fictional “Separator” unit that splits an incoming stream into two or more product streams. The user can specify split fractions for each individual component in the outlet streams, subject to the constraints of the material balance. However, since the split fractions for the various components change during the course of the simulation (due to changing operating conditions), the “Separator” unit could not be simply substituted for the reverse osmosis membrane. With the help of a program called a “task,” though, the problem was solved.

“Tasks” in Aspen Dynamics allow the user to implement changes to a simulation flow sheet in the midst of a running simulation. In the present case, the task was programmed to alter the permeate fraction (permeate flow divided by feed flow to the membrane) and the split fraction of salt in the concentrate stream as a function of feed pressure, composition, and flow rate. The aforementioned empirical model that the task utilized is as follows [37]:

$$P = \left[ a_1 \left( \frac{TMP}{J_F} \right)^{a_2} + a_3 \left( \frac{TDS}{TMP} \right)^{a_4} + a_5 \left( \frac{TDS}{J_F} \right)^{a_6} \right] \quad (8)$$

$$R = \left[ b_1 \left( \frac{TMP}{J_F} \right)^{b_2} + b_3 \left( \frac{TDS}{TMP} \right)^{b_4} + b_5 \left( \frac{TDS}{J_F} \right)^{b_6} \right] \quad (9)$$

Where:

$P$  = Permeate Fraction (%)

$TMP$  = Trans-Membrane Pressure (psi)

$TDS$  = Total Dissolved Solids (ppm)

$J_F$  = Feed Flux to the Membrane (gal/(day·ft<sup>2</sup>))

$R$  = Salt Rejection (%)

$a_i, b_i$  are membrane-specific constants

The model is based on over 500 points of operating data from a commercial 4"x40" membrane, the SWC-1-4040 by Osmotics. The correlations are limited to TDS concentrations of up to 40,000 ppm, transmembrane pressures of 200 to 1,200 psi, and flux ranges of 0.085 to 0.2 GPM/ft<sup>2</sup>. Simulations of the processes were designed to operate within these limitations, to avoid any extrapolations of the model.

Because some of the input parameters for the separator unit differ from those used in the mathematical model, it was necessary to make some conversions. A material balance on the membrane proved useful in finding the equivalence of salt rejection, as given in the above equation, and the corresponding split fraction of salt in the permeate stream that needed to be specified by the task. This analysis and the results can be found in the Appendix, as can be the code for the tasks. Figure 7 is a plot from a simulation run incorporating the task, showing the steady decline in permeate fraction (inner y-axis) that results from the increase in feed salinity mass fraction (outer y-axis) as the batch progresses.

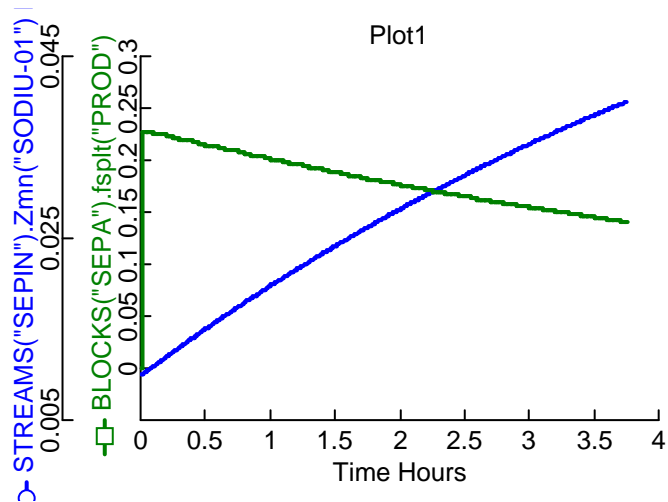


**Figure 7. Aspen Dynamics Plot**

The task also included a correlation for pressure drop across the membrane, feed pressure minus concentrate pressure. The correlation was a fit to data obtained from

simulations conducted in ROSA (Reverse Osmosis System Analysis), Dow Filmtec's membrane system design software, on a 4"x40" membrane comparable to the SWC-1-4040. The correlation, based on 60 data points, gives pressure drop as a function of permeate fraction and feed flow rate. A plot of the data is given in Figure 8. The correlation is:

$$\Delta P = J_F (-0.0106P + 12.9) \quad (10)$$

Where:

$\Delta P$  = Pressure drop (bar)

The correlation coefficient is 0.76. Maximum error (actual minus predicted) for the model was 0.9 psi, or 3%, for the 60-point data set, quite acceptable for the intended purpose of estimating process pumping energy requirements.

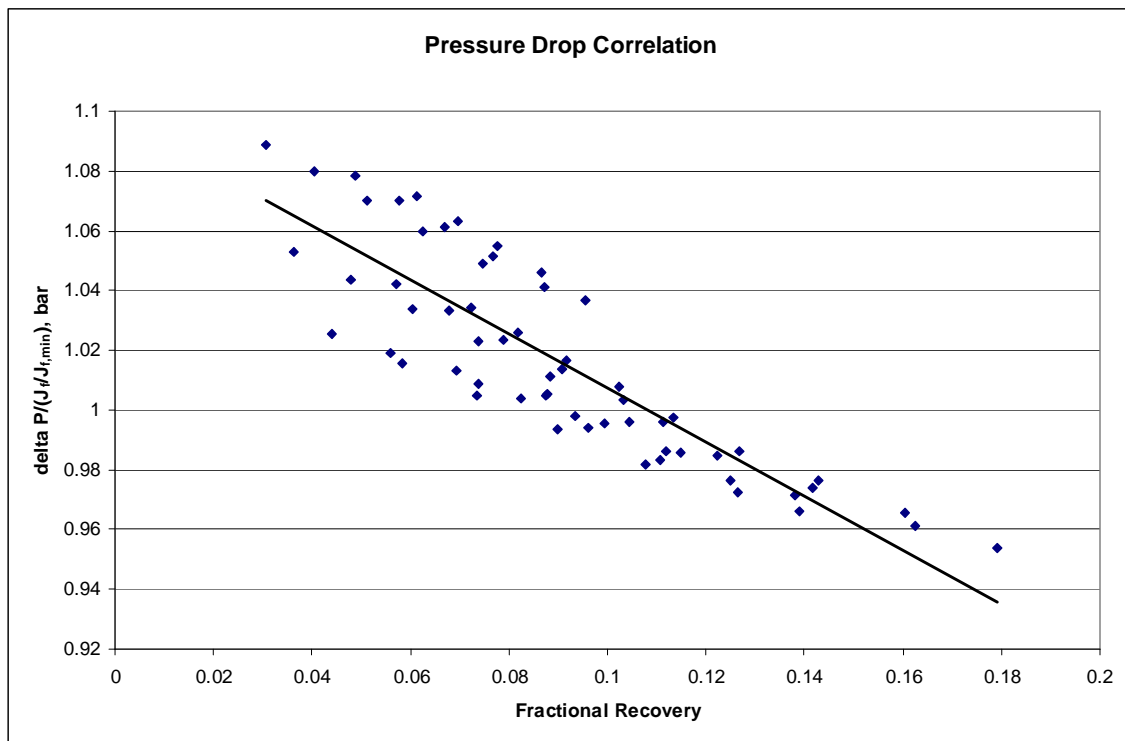


**Figure 8. Membrane Pressure Drop**

A second, simple task was necessary to stop the batch simulation when the desired salinity was reached in the high-pressure tank. All simulations assumed a starting (feed) salinity of 10,000 ppm, with the batch ending when the salinity in the high-pressure tank exceeded 40,000 ppm.

#### 4.1.3 Controller Setup and Tuning

Aspen Dynamics also allows the user to implement controllers in a flow sheet. A PID controller was utilized to control pressure at a set point in the high-pressure tank. The control parameter was inlet feed flow rate. In practice, the manipulated parameter would be the signal to the variable-speed drive of a positive displacement pump, but this was not possible in Dynamics, and manipulating flow rate is essentially equivalent. Dynamics provides default settings for the controller when the user first creates it. However, the default controller settings were found to give highly ideal controller performance, and it was desired to create a more realistic simulation. Process dead time and process time constant are two important characteristics in the dynamics of non-ideal control systems. Their definitions (from Smith [9]) follow.

*Process Dead Time* =  $t_o$  = “finite amount of time between the change in input variable and when the output variable starts to respond”

*Process Time Constant* =  $\tau$  = “Amount of time counted from the moment the variable starts to respond that it takes the process variable to reach 63.2% of its total change”

Once process dead time and time constants were added, simulations showed a rather sluggish control performance. The default tuning settings were very conservative, presumably to avoid controller instability. It was desired to improve the pressure control loop’s tuning. Reasonable tuning parameters for most industrial control loops can be obtained from well-known methods such as Ziegler-Nichols, found in virtually any process control textbook. Online tuning involves obtaining the ultimate gain,  $K_{Cu}$ , by zeroing out the integral (reset) and derivative parameters, then making a step change

with the controller in automatic mode and observing the response. If a continuous oscillatory response results, the current controller gain is the ultimate gain. If not, the gain is changed, a step change is made, the response is observed, and so on until the ultimate gain is found. Once it is found by this trial-and-error process, simple formulas are used to obtain the proportional, integral, and derivative tuning constants [9]. For a PI Controller,

$$K_C = 0.45K_{C,U} \quad (11)$$

$$\tau_I = T_U / 1.2 \quad (12)$$

Where:

$K_C$  = Controller Gain

$K_{C,U}$  = Ultimate Gain

$\tau_I$  = Integral (or Reset) Time (s)

$T_U$  = Ultimate Period (s)

Offline tuning methods are also available to tune a controller. With the controller in manual mode, a step change is made, and the resulting process response curve (plot of process variable versus time) can be used to obtain three process characteristics: *dead time*, *time constant* and

$$\text{Process Gain} = K = \frac{\Delta \text{Output}}{\Delta \text{Input}}$$

Again, simple formulas are used to calculate PID controller tuning parameters from the process gain, dead time, and time constant. For a PI controller, they are:

$$K_C = \frac{0.9\tau}{Kt_o} \quad (13)$$

$$\tau_I = 3.33t_o \quad (14)$$



The pressure loop was tuned with the online method. It was necessary to reduce simulation time steps from the default 0.01 hours to 0.001 hours in order to obtain the desired resolution, since dynamic fluctuations are rather rapid when introducing perturbations into the process.

One control characteristic of note is the loop's increasingly strong reaction to flow changes as the level in the tank increases. In process control language, the higher the tank level, the higher the process gain. When the tank is initialized to 125 psi, and then filled with water to a typical operating pressure of 1000 psi, the tank is nearly 90% full, and pressure is very sensitive to changes in level. While initializing the tank to a higher pressure would reduce this high sensitivity and process gain, cost of initialization would rise substantially, with higher energy costs, as well as higher capital costs for higher-pressure compressors.

The second control loop in the process is a flow loop. This simple loop, containing a pump operating at constant speed, contains a control valve to maintain the desired flow to the membrane. A flow transmitter provides the input signal to the controller. Because such loops have a rapid control response, the flow in the loop was considered constant, and flow to the membrane was fixed at the desired rate in the simulation.

Smith [9] explains tuning consideration for flow loops. Normally, dead time for flow loops containing control valves is minute. Since dead time appears in the denominator of tuning equations for controller gain (for all methods), these equations predict a gain approaching infinity, a meaningless result. In fact, the integral action is what is necessary in tuning flow loops. For a PI controller, Smith makes the following recommendations for conservative and aggressive settings:

Conservative:  $K_c = 0.1$ ,  $\tau_I = 0.1$  minutes

Aggressive:  $K_c = 0.2$ ,  $\tau_I = 0.05$  minutes

These settings provide 10 and 20 times more integral action than proportional, respectively.

The flow control loop could be considered an “optional accessory” to the process under consideration. If it was absent, flow to the membrane would fluctuate somewhat throughout the duration of the batch, but provided the recycle pump was properly sized, the flow rates would not be so high as to damage the membrane. In fact, the higher flow rates that would occur in the absence of a control valve would probably enhance membrane performance, due to reduced concentration polarization.

#### 4.1.4 Configuring Aspen Dynamics for Process Simulation

A number of default settings in Aspen Dynamics must be changed to run a simulation successfully. The following is the procedure to convert a newly exported file from Aspen Plus into a functional simulation.

1. Make the changes listed in Tables 1-3 in the “All Variables” table of the appropriate block or stream (NC = No Change):

**Table 1. Mixer (High-Pressure Tank) Parameter Settings**

Parameter	Description	Spec: Default	Spec: New	Value
E	Internal Energy	Fixed	Free	NC
Fml_outR	Specified Liquid Flow Rate	Fixed	Free	NC
Level	Liquid Level	Free	Initial	0.01 ft *
Mc	Comp Molar Holdup	Initial	Free	NC
P	Pressure	Free	Initial	125 psi **
T	Temperature	Free	Initial	95°F **
x(“water”)	Liquid Mole Fraction	Free	Fixed	0.9969 ***

\* For starting the simulation with the tank empty of liquid. An error message was obtained when using a value of zero. If it is desired to start a simulation from the point at which the tank is full and the pressure has reached operating pressure, level and pressure should be specified accordingly.

\*\* These values were used in the simulation runs, but can be other values as the user desires.

\*\*\* This value corresponds to initial salinity of 10,000 ppm.

**Table 2. Separator (RO Membrane) Parameter Settings**

Parameter	Description	Spec: Default	Spec: New	Value
Fsplit("Perm")	Outlet Flow Split Fraction	Free	Fixed	NC*
P("Conc")	Pressure	Fixed	Free	NC
P("Perm")	Pressure	Fixed	NC	15 psia
P_drop("Conc")	Pressure Drop	Free	Fixed	NC*
Sfrac("Conc", "Nitrogen")	Component Flow Rate Split Fraction	Free	Fixed	NC
Sfrac("Conc", "Sodium-01")	Component Flow Rate Split Fraction	Free	Fixed	NC*

\* The ROsimulator task sets these values during the course of the simulation.

**Table 3. Streams Parameter Settings**

Stream	Parameter	Description	Spec: Default	Spec: New	Value
Inlet to Separator	Fv	Total Volume Flow	Free	Fixed	10 gpm*
Inlet to Process	FvR	Specified Total Volume Flow	Fixed	Free	NC**

\* Sets the flow rate to the RO / Separator. Values of 6-12 gpm used in simulations.

\*\* Manipulated variable for the pressure controller

2. Set up the tasks necessary for the simulation. To add a task, select "Flowsheet" from the All Items pane of the exploring window, then double click on the "Add Tasks" icon in the "Contents of Flowsheet" pane. The code for the "ROsimulator" and "PauseIt" tasks are given in the Appendix. Double-clicking the icon for each task activates it so that it will run automatically upon starting the simulation. Activation is indicated with a blue check mark appearing over the each task's icon.

3. Configure the pressure controller. By default, Dynamics includes a pressure controller and level controller for the Mixer block. The level controller is unnecessary and should be deleted. The controller output stream should be reconnected to the process inlet stream, with "Fv" selected as the manipulated parameter. If a more realistic controller performance is desired, "Deadtime" and "Lag\_1" ControlMode blocks can be added to

the loop to include dynamic characteristics of the control elements. Regardless of whether the additional blocks are included, several specifications must be made for the controller in its “Configure” form.

- a. Set Point (“Tuning” tab): Values of 600 – 1200 psia used in simulation runs
- b. Controller Action (“Tuning” tab): change from “Direct” to “Reverse”
- c. Process Variable and Setpoint Minimum (“Ranges” tab): 0 psia
- d. Process Variable and Setpoint Maximum (“Ranges” tab): 1500 psia (or perhaps lower – in practice this would be limited by pressure transmitter maximum, pressure relief valve setting, or vessel maximum pressure)
- e. Output Minimum (“Ranges” tab): 0 ft<sup>3</sup>/hr
- f. Output Maximum (“Ranges” tab): 30 ft<sup>3</sup>/hr. This value is limited by the flow capacity of the pump, or residence time requirements for the organo-clay adsorbent pretreatment.

#### 4.1.5 Calculating Process Energy Requirements

In simulation results, Aspen Dynamics gives power consumption for the pumps in the process. Power is given as electrical power, brake power, and fluid power. Electrical power represents that delivered to the motor of the pump. Brake power is the portion of the power that the motor delivers to the pumping mechanism (i.e. impeller). Fluid power is the portion of the power that actually increases the mechanical energy of the fluid. Mathematically, they are related as follows:

$$P_e = \frac{P_b}{\eta_m} = \frac{P_f}{\eta_h \eta_m} \quad (15)$$

Where:

$P_e$  = electrical power

$P_b$  = brake power

$P_f$  = fluid power

$\eta_m$  = motor efficiency

$\eta_h$  = hydraulic efficiency

It was anticipated that the power consumption indicated in Aspen Dynamics could be used directly to find the processes' energy requirements. Unfortunately, there were some irregularities in Aspen that prevented this simple approach. Specifically, the simulator permitted streams to flow into the pressure vessel that were at a pressure below that of the vessel. Presumably, this is because the simulation was being conducted in "Flow Driven" mode instead of "Pressure Driven" mode, so rigorous pressure-flow relationships were not enforced. However, it was not possible to change to "Pressure Driven" mode since that mode disallows the use of the "Separator" unit, the fictional unit used to simulate the reverse osmosis membrane. Therefore, pump energy requirements were estimated using stream flow rates from the dynamic simulations, required pressure boosts for the streams throughout the process, and assumed pump efficiencies. The relationship is as follows:

$$P_f = Q\Delta P \quad (16)$$

Where:

$Q$  = Volumetric flow rate

$\Delta P$  = Pressure increase across pump

Aspen Dynamics users can obtain parameter values for each step in a simulation run via the Table or History Table functions. The Table function was used to obtain flow rates through both the high-pressure feed pump and the recycle pump. During the initialization phase for the batch, when the high-pressure tank is filling with liquid and approaching RO operating pressure, flow rate is constant and pressure increase varies with time. The recycle pump has no power requirement since it is off. Once operating pressure is reached and the reverse osmosis process proceeds, pressure increase for the feed pump is approximately constant, with an inlet pressure of atmospheric, and an outlet pressure of 600 to 1200 psia. Flow varies with time, gradually decreasing as the batch proceeds. The variable-speed drive slows down, lessening power demand. The recycle pump's flow gradually increases with time, to maintain a constant feed flow to

the membrane. It is assumed to operate at constant power, with a control valve in place to regulate flow rate. The pump is sized for the highest flow and pressure boost, and likewise the power is calculated as constant for the greatest flow and pressure boost during the batch cycle, regardless of transient conditions.

The energy consumed during each batch was calculated as the sum of the time integral of fluid power for the initialization and RO operating phases, divided by pump efficiency. An efficiency of 60% was assumed. Darby [38] gives typical peak pump efficiencies of 50% to 90%, so 60% was chosen as an intermediate value.

$$\eta_{pump} = \eta_h \eta_m = 0.60$$

$$\text{Batch Pumping Energy} = \frac{\int P_f dt}{\eta_{pump}} \approx \frac{\sum_{i=1}^m (P_{f,hpp} + P_{f,rcy}) \Delta t_1 + \sum_{j=1}^n (P_{f,hpp} + P_{f,rcy}) \Delta t_2}{0.60} \quad (17)$$

Where:

$P_{f,hpp}$  = Fluid power imparted by high-pressure feed pump

$P_{f,rcy}$  = Fluid power imparted by recycle pump

$$m = \frac{\text{duration of initialization}}{\text{time step} = \Delta t_1}$$

$$n = \frac{\text{duration of desalination}}{\text{time step} = \Delta t_2}$$

## 4.2 Simulation Results

### 4.2.1 Optimization

Figure 9 compares the pumping energy consumption of the original and modified (single membrane) processes, at various operating pressures. Operating conditions and assumptions are as follows: 10,000 ppm inlet feed, batch ending when concentrate

reaches 40,000 ppm, 95°F feed temperature, 8 gpm flow to the membrane = 0.11 gpm/ft<sup>2</sup> flux, 60% pump efficiency.

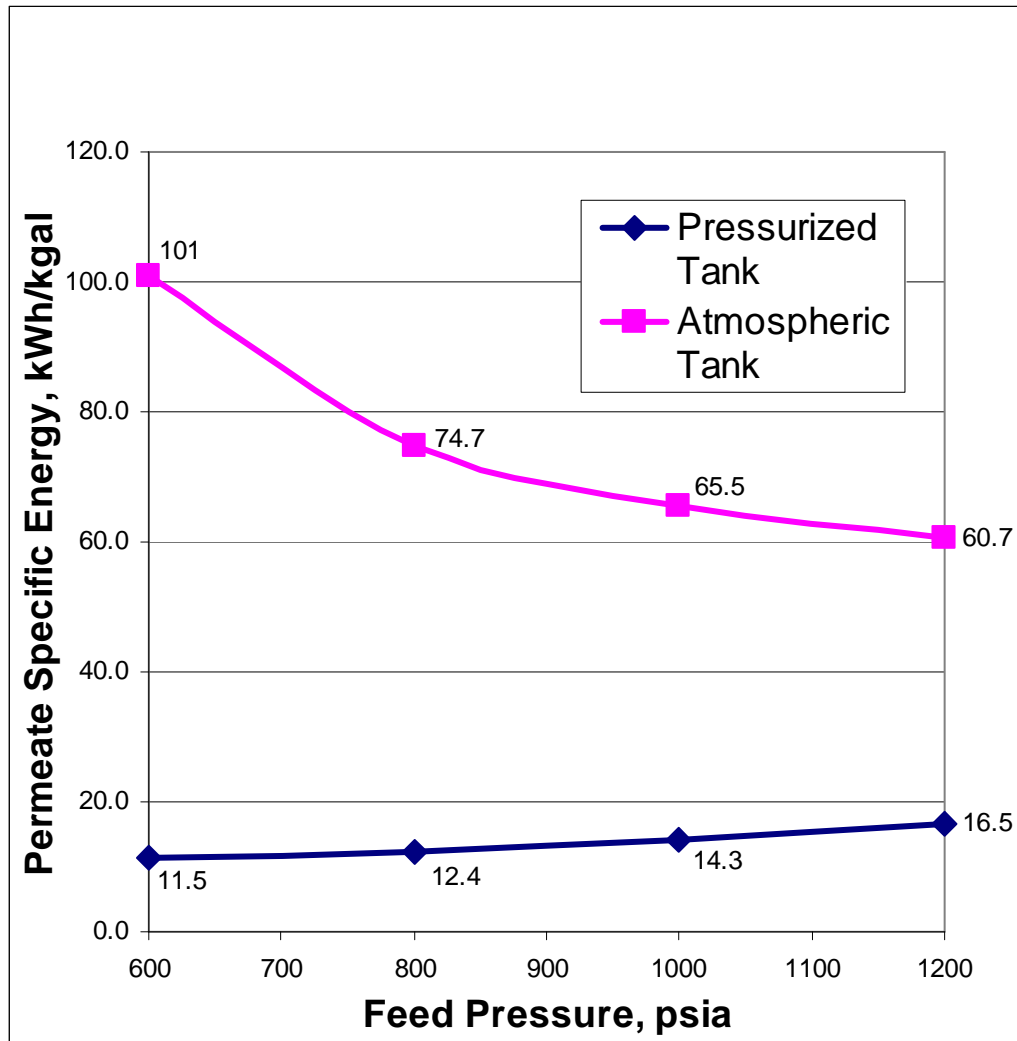


**Figure 9. Energy Consumption Comparison**

As the figure indicates, pumping energy requirements for the modified process in which concentrate is recycled to a pressurized vessel are a fraction of the original.

A comparison of specific energy requirements at various feed flux rates is given in Figure 10. The data given are for the modified process with pressurized recycle, under the same assumptions as in the previous figure.

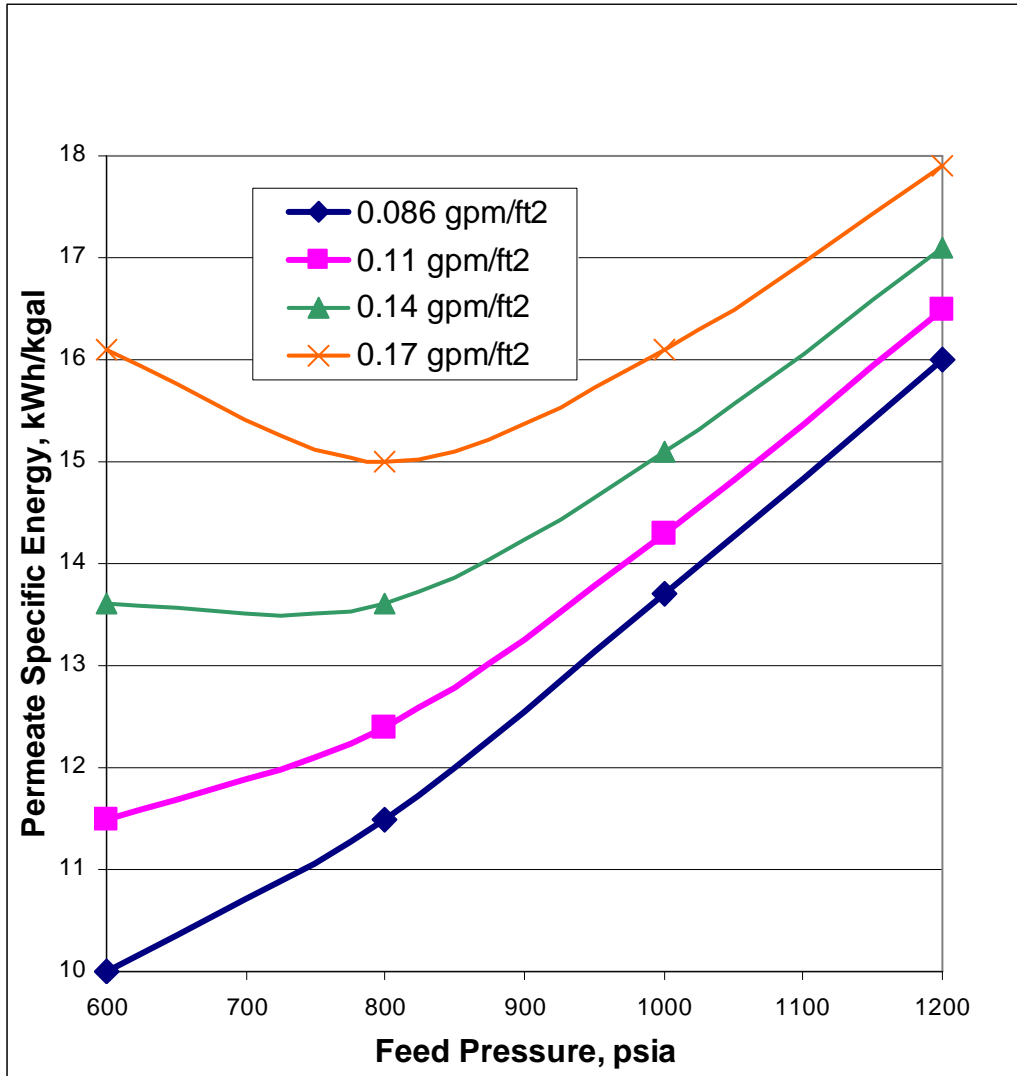


**Figure 10. Energy Consumption, Various Feed Fluxes**

Direct comparison between the “membranes in series” configuration and the recycle arrangements are difficult since the desalting endpoint cannot be fixed at 40,000 ppm, or any other arbitrary salinity. For this reason, results from simulations of series arrangements could not be included in Figure 9. Table 4 gives results from the series configuration in tabular format.



**Table 4. Energy Consumption, Series Configuration**

<b>Feed TDS, ppm</b>	<b># of Memb.</b>	<b>Feed Press., psia</b>	<b>Feed Flux, gpm/ft<sup>2</sup></b>	<b>Recovery</b>	<b>Conc. TDS, ppm</b>	<b>Specific Energy, kWh/kgal</b>
10000	4	800	0.17	42.8%	17300	13.3
10000	4	1000	0.17	53.3%	21100	13.4
10000	4	1200	0.17	62.3%	26000	13.8
10000	4	800	0.20	37.6%	15900	15.2
10000	4	1000	0.20	47.2%	18700	15.1
10000	4	1200	0.20	55.8%	22200	15.4
10000	6	800	0.17	58.7%	23700	9.7
10000	6	1000	0.20	64.3%	27400	11.1
10000	6	800	0.20	52.6%	20700	10.8
20000	4	800	0.17	34.9%	30200	16.3
20000	4	1000	0.17	46.4%	36500	15.4
20000	4	1200	0.17	56.5%	44600	16.9
20000	4	800	0.20	30.5%	28400	18.7
20000	4	1000	0.20	40.9%	33300	17.4
20000	4	1200	0.20	50.3%	39300	17.1
20000	6	800	0.17	47.0%	36800	12.1
20000	6	1000	0.20	55.7%	43700	12.8
20000	6	800	0.20	41.7%	33500	13.6

The results indicate that energy savings for a series configuration are similar to those for the pressurized recycle arrangement – both typically having specific energy requirements of 10 – 20 kWh/kgal permeate.

To weigh the operating cost savings due to reduced energy consumption versus the additional capital costs to modify the process to the pressurized recycle configuration from the existing design, a case study was carried out. In the case study, a unit is equipped with a single, 8”x40” RO membrane, assumed to be operating for 12 hours per day, running batches one after the other. Feed flux is 0.11 gpm/ft, feed pressure is 1000 psia, with feedwater salinity of 10,000 ppm, so based on simulation results the unit would process an average of 460 gallons per hour of produced water during the 12 hours. About 350 gallons of this is recovered as permeate. Capital costs for the additional pump, pressure vessel, and control valves were estimated from correlations in

Peter, Timmerhaus, and West [39]. Costs of other items in Table 5 were estimated based on internet-advertised prices, as of 2006.

**Table 5. Additional Capital Costs, Pressurized Recycle Configuration**

<b>Item</b>	<b>Cost</b>
Pressure Transmitter	\$300
Flow Transmitter	\$1,000
Control Valve, 2", SS	\$1,000
Control Valve, 1", SS	\$1,800
PLC w/PID capability	\$600
Lined Pressure Vessel (110 gal)	\$9,000
Pump, Stainless Steel	\$5,400
Piping, misc.	\$900
<i>Total Additional Cost:</i>	<i>\$20,000</i>

From Figure 9, the energy consumption difference between the original and modified processes is 51.2 kWh/kgal permeate. Assuming an energy cost of \$0.20/kWh,

$$51.2 \text{ kWh/kgal} \times \$0.20/\text{kWh} = \$10.24/\text{kgal}$$

$$\$20,000 / (\$10.24/\text{kgal}) = 1950 \text{ kgal permeate produced to break even}$$

$$0.35 \text{ kgal/hr} \times 12 \text{ hr/day} = 4.2 \text{ kgal permeate per day}$$

$$1950 \text{ kgal} / (4.2 \text{ kgal/day}) = 465 \text{ days}$$

So, neglecting the time value of money, the operating cost savings will equal the additional capital expenditure at about 15 months of operation. As can be inferred from the above calculation, payoff period is directly proportional to energy cost, so doubling the energy cost to \$0.40/kWh would halve the payoff period to 233 days.

#### 4.2.2 Process Control

The general strategies for control of the processes are shown in Figures 11 and 12 and Table 6.

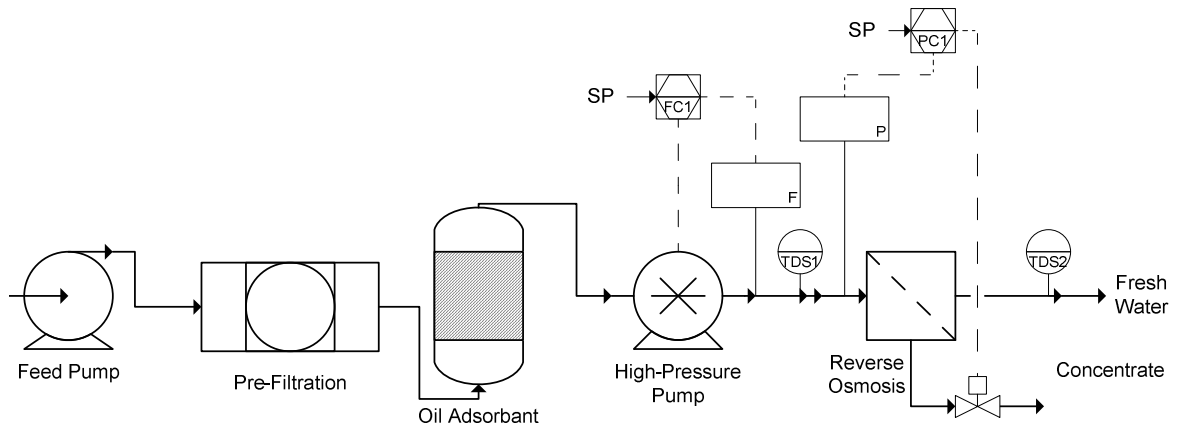


**Figure 11. Original / Series Control System**

The control arrangement in the series configuration is conceptually identical, with the control valve being placed on the concentrate stream of the final membrane in the series. In either case, the concentrate would most likely be recycled to the feed tank to increase recovery, although not depicted in the drawing.

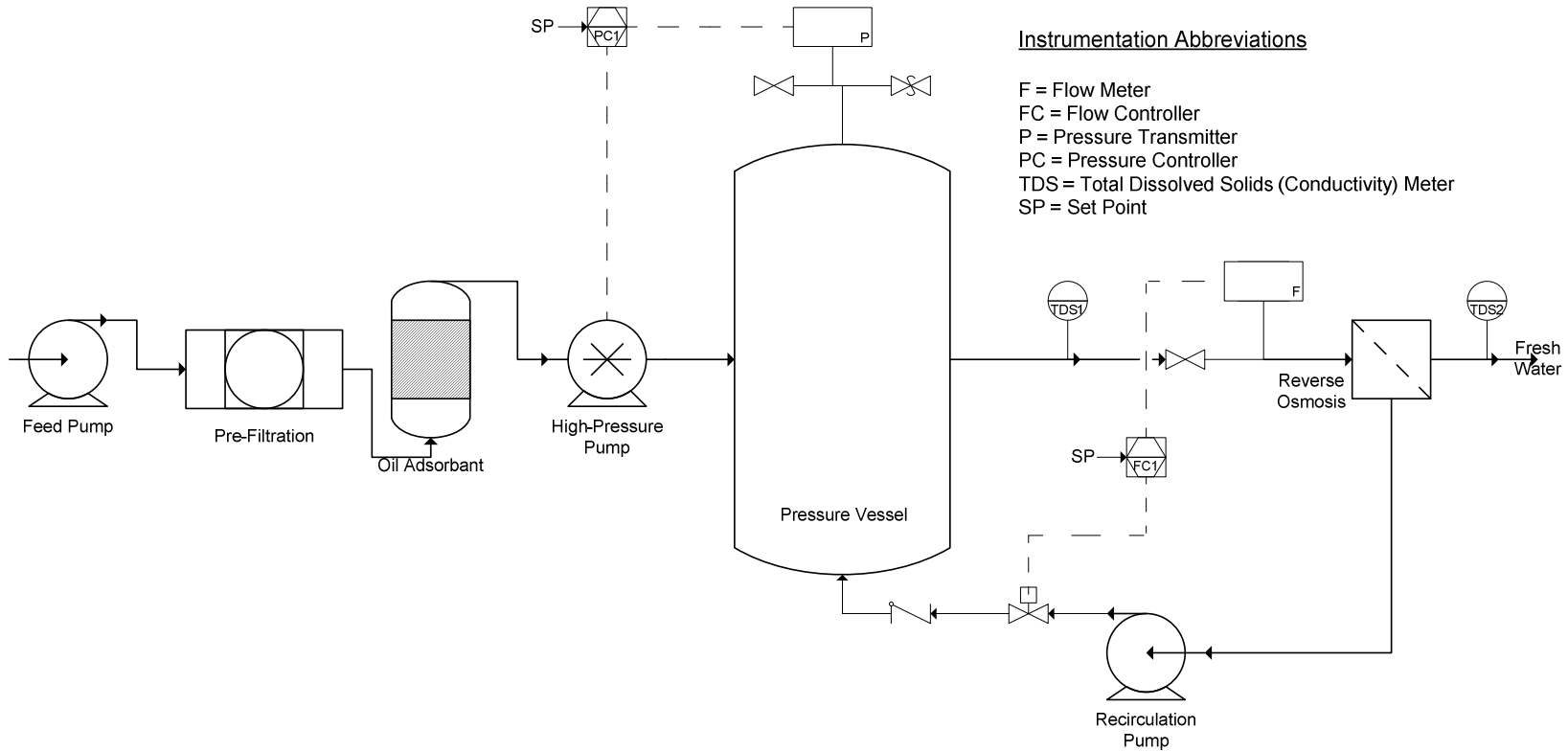


**Figure 12. Pressurized Recycle Control System**

**Table 6. Control Overview**

	<b>Controlled Variable</b>	<b>Manipulated Parameter</b>	<b>Set Point</b>	<b>Batch End Point</b>	<b>Startup</b>	<b>Shutdown</b>	
<b>Original Process</b>	Feed Pressure	Valve position on concentrate stream	Fixed, or cascaded from permeate TDS meter	Feed or permeate reaches upper salinity limit, or scaling mineral concentration reaches upper limit	N/A	Feed tank drained of residual (waste)	
	Feed Flow Rate	High pressure pump motor speed	Fixed				
<b>Membranes in Series</b>	Feed Pressure	Valve position on concentrate stream	Fixed, or cascaded from permeate TDS meter				
	Feed Flow Rate	High pressure pump motor speed	Fixed				
<b>Pressurized Recycle</b>	Feed Pressure	High pressure pump motor speed	Fixed, or cascaded from permeate TDS meter		Tank charged with pressurized air, then water flows in to increase pressure to set point		Pressurized tank drained of residual
	Feed Flow Rate	Valve position on recycle stream, or no control	Fixed, or no control				

The pressure control loop in the pressurized recycle process differs from typical pressure controllers in RO plants, and thus warranted further study. The following table shows results from an analysis intended to find the dependence of the loop's tuning parameters on initialization and operating pressures. The process gains were determined from Aspen Dynamics simulations, under the following conditions: controller loop time constant and deadtime of 6 seconds each, process variable range of 0-1500 psi, controller output (flow through high-pressure pump) 0-3.74 gpm, high pressure tank vertical with a 2-foot diameter and 5-foot height, and a single 4"x40" RO membrane.

**Table 7. Controller Gain**

<b>Initialization Pressure, psia</b>	<b>Operating Pressure, psia</b>	<b>Ultimate Gain, <math>K_u</math>, %/%</b>	<b>Controller Gain, Z-N Method</b>
62.5	600	150	68
62.5	800	100	45
62.5	1000	53	24
125	600	400	180
125	800	180	81
125	1000	130	59
250	600	700	315
250	800	500	225
250	1000	300	135

The ultimate period for all of the above configurations was approximately constant for each case tested, at about 40 seconds, resulting in an integral (reset) time of 48 seconds using Ziegler-Nichols formulas for a proportional-integral controller. As expected, higher gains were calculated for higher initialization pressures and lower operating pressures – cases in which there was greater vapor space in the pressure vessel and thus less pressure sensitivity. Attempts to determine the gains for an operating pressure of 1200 psia were unsuccessful due to convergence problems with the simulator.

Figures 13 and 14, below, show a process tuned at its ultimate gain, then re-tuned using the Ziegler-Nichols rules, respectively.

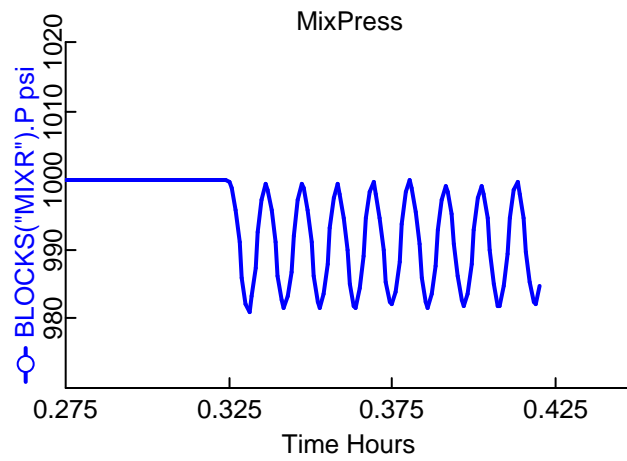


**Figure 13. Finding Ultimate Gain**

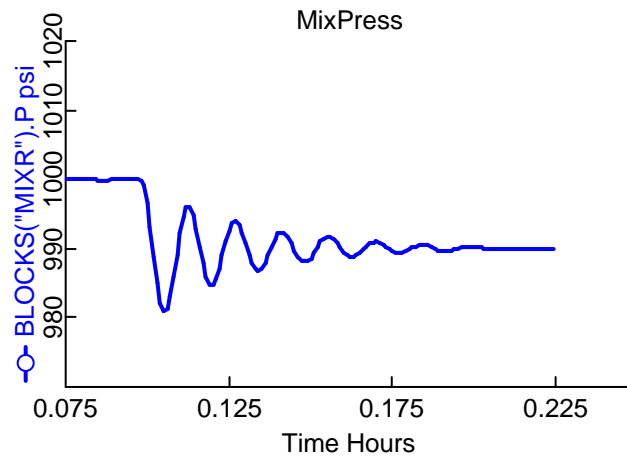


**Figure 14. After Z-N Tuning**

## **5. EVALUATION OF POTENTIAL RENEWABLE ENERGY USE**

While the literature review section included reviews of some desalination systems that did not require electricity generation, such configurations are not compatible with the existing process designs, which utilize electrically-driven pumps, and will most likely include a control system which also requires electricity. Therefore, electrical power is a prerequisite for operation of the treatment process. For remote sites far from the power grid, various generating methods are available. The best-established and most obvious option, portable, fossil-fuel-burning generators, was evaluated first as the baseline option. Then, wind- and sun-powered generation was evaluated.

### **5.1 Diesel Generation**

As compared with wind and solar generation, diesel generators have a low initial cost and high operating cost. Fuel consumption is the major operating cost. With prices for petroleum escalating rapidly in recent years as indicated in Figure 15, and with little likelihood of a downward trend, this is clearly the major drawback to the use of diesel generators.





**Figure 15: US Retail Diesel Prices**

One advantage of diesel generators is that since they have been in use for decades, their operating characteristics are well-known. Having many moving parts and being relatively mechanically complex, they require regular maintenance to sustain operability. According to Jimenez, a well-maintained diesel generator will typically have a lifetime of 25,000 operating hours. Table 8 contains a cost estimate for diesel-generated electricity, based on a 25,000-hour life and other guidelines given in [40].

**Table 8. Diesel-Generated Electricity Costs**

<b>Size (kW)</b>	<b>Capital + O&amp;M Costs (\$/kWh)</b>	<b>Fuel Price (\$/gal)</b>	<b>Fuel Cost (\$/kWh)</b>	<b>Total Cost (\$/kWh)</b>
5 to 10	0.11	2	0.21	0.32
		3	0.32	0.43
		4	0.42	0.53
20 to 50	0.05	2	0.19	0.24
		3	0.29	0.33
		4	0.38	0.43

## 5.2 Renewable Sources

Both wind energy and solar energy were considered as renewable energy sources for the water treatment unit. The power system would have to include electricity storage, and lead-acid batteries were chosen over nickel-cadmium due to lower cost. The method chosen for sizing PV arrays and battery banks is one developed by Sandia National Laboratories' Photovoltaics Systems Program. The method is published in "Stand-Alone Photovoltaic Systems: a Handbook of Recommended Design Practices" in worksheet format [41]. Since numerous sites were to be evaluated, a macro-driven Microsoft Excel spreadsheet was developed to automate the method and allow the user to choose from several site locations, battery types, PV panels, and other options. Additionally, the spreadsheet allows the user to input data for custom sites, batteries, and solar panels, if desired. For wind turbine sizing, the spreadsheet links to a Microsoft Excel simulator for a popular battery charging wind turbine, the Bergey Excel. The simulator was obtained from the Bergey Company, and is available from their website[42]. Wind and solar data was obtained from [43], [44] respectively.

Following is a list of input cells that must be completed by the user of the Renewable Energy System Sizing Excel Spreadsheet, as well as a screen shot of the program (Figure 16):

Cell B6: The user selects a site from the drop down list, or selects “other” and can input altitude, and wind and solar resource data for a custom site into the dialog box that appears.

Cell B7: The user chooses whether he would prefer the calculations be made from annual average wind and solar data, or, more conservatively, from the lowest monthly average wind and solar data.

Cell B15: Daily electrical load, in kilowatt hours

Cell B16: System Voltage, selected from a drop-down menu of common voltages

Cell B17: Converter Efficiency, defined as power in divided by power out, for the DC to AC inverter. The default value, as suggested in Sandia’s handbook, is 85%.

Cell B18: Wire Efficiency, accounting for power losses due to resistance in the wiring. The default value is 98%.

Cell B22: Required Availability. The user selects 95% or 99% from the drop-down list. The number of battery storage days is the calculated as a function of the required availability.

Cell B23: Battery make and model is selected from a drop-down list, or “other” is selected and the user inputs battery performance parameters into a dialog box. Input required is battery voltage, amp-hour capacity at 20-hour discharge rate, weight (lbs), and price (\$).

Cell B28: Maximum Depth of Discharge, the percentage of usable capacity in the battery. Recommended value for deep-cycle batteries, including all found in the

drop-down list in cell B23, is 75%. Discharging much beyond this value can severely shorten battery life.

**Renewable Energy System Design Tool**

**Instructions:** Complete all **Yellow** Cells

**Input Information**

**Site**

Location: Amarillo

Base Calculations on Average Annual Wind

Lowest Monthly Average Wind

Average Annual Insolation

Lowest Monthly Avg Insolation

**Electrical System**

Load: 16 kWh/day

Voltage: 48 Volts

Converter Efficiency: 85%

Wire Efficiency: 98%

**Battery Bank**

Required Availability: 95%

Make & Model: Surrette 6CS 17PS

Model Voltage: 6 Volts

Model Capacity (20hr dischrg): 546 Amp Hours

Model Weight: 221 lbs

Model Price: \$650

Max Depth of Discharge: 75%

Efficiency (Pwr In / Pwr Out): 90%

Temperature Derating: 95%

**PV Array**

Make & Model: BP 380-U

Rated Module Current: 4.55 Amps

Hi Temp Max Voltage: 16 Volts

Unit Weight: 17 lbs

Unit Area: 6.84 ft<sup>2</sup>

Unit Price: \$474

Derating Factor: 95%

**Bergey Excel Wind Turbine**

Derating Factor: 90%

**Output Information**

Load: 392.2 AH

Corrected Load: 444.6 AH

Design Current: 70.0 A

Storage Days: 3 Days

Required Capacity: 1872.1 AH

Number in Parallel: 4

Number in Series: 8

Total Batteries: 32

Total Weight: 7,072 lbs

Total Cost: \$20,800

Derated Design Current: 73.7 A

Modules in Parallel: 17

Modules in Series: 4

Total Modules: 68

Array Weight: 1156 lbs

Array Area: 465.12 ft<sup>2</sup>

Array Cost: \$32,232

Daily Energy Output: 48.7 kWh/day

Output-to-Load Ratio: 3.0

Figure 16. Renewable Energies Spreadsheet

Cell B29: Battery Efficiency, defined as energy into the battery divided by energy leaving the battery. All batteries lose some power during the charge/discharge cycle due to waste heat, etc. Default value is 90%.

Cell B30: Temperature derating, to account for the reduction in efficiency due to low operating temperatures. Sandia recommends obtaining this information from the manufacturer, or otherwise derating the capacity by one percent for each degree Celsius below 20°C. The default value is 90%.

Cell B34: Select a make and model of photovoltaic panel, or select “other” and input the required parameters in the dialog box. “Rated Module Current” is current, in amperes, when operating with 1 kW/m<sup>2</sup> insolation and 45°C. “Hi Temp Max Voltage” is the panel’s output voltage when operating at the highest foreseeable temperature. Price (\$), panel weight (lbs), and panel area (ft<sup>2</sup>) are also inputted via the dialog box for custom panels.

Cell B40: Derating factor, to compensate for the reduction in power output from the PV array due to dust accumulation, aging, etc. Default value is 90% for crystalline silicon panels.

Cell B44: Wind turbine derating factor, to account for unusable energy such as when batteries are full, and otherwise as a safety factor. Default value is 90%.

Output results from the spreadsheet include:

- Number and arrangement of storage batteries and PV panels
- Battery and PV panel weight
- Battery and PV panel cost
- Wind turbine energy output

Additionally, site characteristics are listed, specifications for the various system components are given, along with design characteristics such as design current. The spreadsheet was used to evaluate several Texas locations for their renewable energy potential. Wind and solar energy costs are given in Figures 17 and 18, respectively.

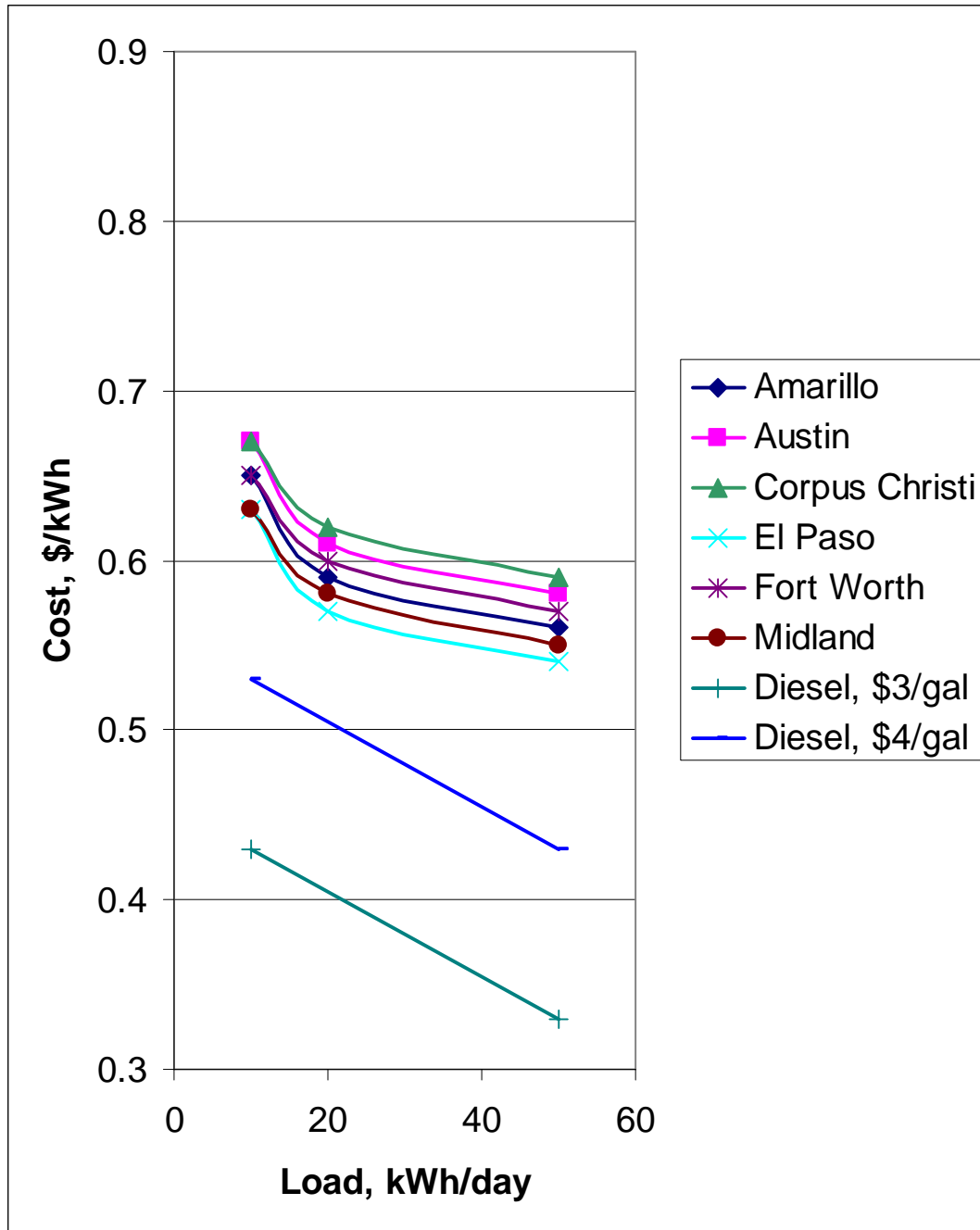


Figure 17. Solar Energy Costs

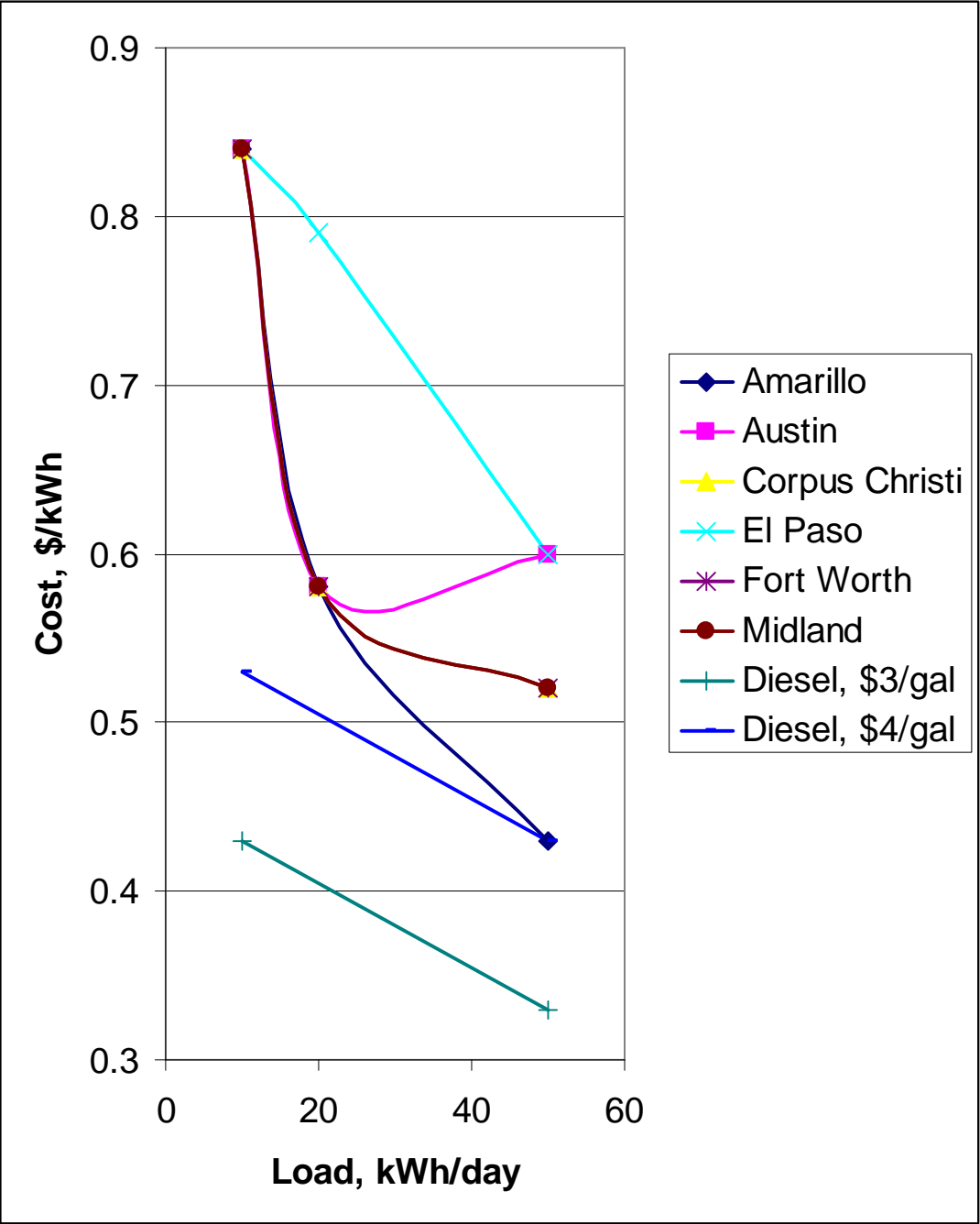


Figure 18. Wind Energy Costs

By way of explanation, the Wind Energy Costs figure appears to show some inconsistency in the cost trend for some of the cities. The step-like descent in costs

results because if a single wind turbine was insufficient to meet a given load, a second or third had to be added, greatly ballooning costs over a short range of load.

The figures show that the cost of renewable energies in the present application, rather small in scale and with a need for expensive battery storage, is somewhat higher than that of diesel-generated electricity. However, even with this disadvantage, wind-generated electricity is cost-competitive with diesel generated electricity in wind locales such as Amarillo at loading levels of 50 kWh/day.



## 6. CONCLUSIONS AND RECOMMENDATIONS

The process optimization efforts yielded great gains in energy efficiency. Over the full range of operating conditions, the pumping energy requirements, which constitute nearly all of the process' energy consumption, are reduced to less than 1/3 of the original levels. As shown in the case study in Section 4, the savings are easily great enough to justify the additional capital expenses, with a payback time under 1.5 years for a 460 gph treatment process.

The process control schemes developed and outlined in Section 4 utilize simple, robust feedback control. The most complicated scheme, for the pressurized recycle configuration, was successfully implemented in dynamic simulations, and tuning parameters were calculated for the pressure loop. The results from the tuning exercise are clearly tentative, however, since accurate tuning parameters can only be determined when dynamic characteristics such as deadtime and gain for the actual equipment are known. In other words, final tuning must be done on the physical process itself, not with a computer simulator.

Results from the renewable energy analysis were generally disappointing, but do show potential for using wind energy to power the process in areas with Class 4 winds such as the Texas Panhandle. At higher loads, in the 50 kWh-per-day range, cost was approximately equal to that of diesel-generated electricity using \$4 per gallon diesel. The trend indicated, however, that at higher loadings the cost of wind energy would dip well below that of diesel-generated power. Future researchers may also consider the combined use of wind, solar, and/or diesel sources in a hybrid system. Such combinations normally allow for less battery storage and therefore potentially lower cost.

It is recommended that much more pilot testing be carried out to determine the susceptibility of the RO membrane to fouling. Chemical, physical, and biological fouling are all possible in the processes presented in this thesis, and an extended operational study treating a produced water of typical composition would aid in determining the

likelihood and speed of fouling. This is a factor that has a great influence on the economics of reverse osmosis processes, due to the high cost of membrane replacement.

As part of the membrane fouling study, various options for pretreating the water could be explored, such as the addition of antiscalant chemicals and biocides. Finally, procedures should be developed for cleaning the membranes when fouling does occur. The explanation and literature review of fouling phenomenon provided in this thesis testifies to the difficulty of maintaining clean membranes.

## REFERENCES

1. C.T. Kiranoudis, N.G. Voros, and Z.B. Maroulis, Wind Energy Exploitation for Reverse Osmosis Desalination Plants, *Desalination* 109 (1996) 195-209.
2. C. Patel, Management of Produced Water in Oil and Gas Operations, M.S. Thesis in Petroleum Engineering. 2004, Texas A&M University, College Station.
3. M.T. Stephenson, A Survey of Produced Water Studies, in *Produced Water*, J.B. Ray and F.R. Engelhardt, Editors. Plenum Press, New York 1992.
4. B.R. Hansen and S.R.H. Davies, Review of Potential Technologies for the Removal of Dissolved Components from Produced Water, *Trans IChemE* 72 (1994) 176-188.
5. M.A. Siddiqui, Sustainable Development through Beneficial Use of Produced Water for the Oil and Gas Industry, M.S. Thesis in Petroleum Engineering. 2002, Texas A&M University, College Station.
6. Texas Renewable Energy Resources: Wind. Texas State Energy Conservation Office [accessed 2006 April 20]; Available from: <http://www.infinitepower.org/reswind.htm>.
7. Texas Operational Wind Plants (As of 2/06). Texas Renewable Energy Industries Association [accessed 2006 April 20]; Available from: [http://www.treia.org/pdf\\_files/Wind%20Plant%20Chart.pdf](http://www.treia.org/pdf_files/Wind%20Plant%20Chart.pdf).
8. T.N. Eisenberg, *Reverse Osmosis Treatment of Drinking Water*. Butterworths, Boston, 1986.
9. C. Smith, *Automated Continuous Process Control*. Wiley, New York, 2002.
10. Y.A. Abakr and A.F. Ismail, Theoretical and Experimental Investigation of a Novel Multistage Evacuated Solar Still, *Journal of Solar Energy Engineering* 127 (2005) 381-385.
11. D. Taylor, Wind Energy, in *Renewable Energy: Power for a Sustainable Future*, G. Boyle, Editor. Oxford, Glasgow, 2004.
12. E. Hau, *Windturbines : Fundamentals, Technologies, Application and Economics*. Springer, New York, 2000.

13. American Heritage Dictionary of the English Language. 4th ed. Bartleby Com., New York, 2000.
14. M. Chaplin, Filtration. 2004, London South Bank University [accessed 2005 October 28]; Available from: <http://www.lsbu.ac.uk/biology/enztech/filtration.html>.
15. Separation Ranges. 2005, Koch Membrane Systems [accessed 2005 October 30]; Available from: [http://www.kochmembrane.com/ps\\_exmem.html](http://www.kochmembrane.com/ps_exmem.html).
16. R. Bergman, Membrane Processes, in Water Treatment Plant Design, E. Baruth, Editor. McGraw-Hill, New York, 2005.
17. The Process of Reverse Osmosis. Tiger Purification Systems [accessed 2005 October 28]; Available from: [http://www.watertiger.net/RO/how\\_ro\\_works.htm](http://www.watertiger.net/RO/how_ro_works.htm).
18. D. Potts, R.C. Ahlert, and S.S. Wang, A Critical Review of Fouling of Reverse Osmosis Membranes, *Desalination* 36 (1981) 235-264.
19. J. Lepore and R.C. Ahlert, Fouling in Membrane Processes, in Reverse Osmosis Technology. Marcel Dekker, New York, 1988.
20. H. Ridgway and H. Flemming, Membrane Biofouling, in Water Treatment Membrane Processes. McGraw-Hill, New York, 1986.
21. R. Funston, R. Ganesh, and L. Leong, Evaluation of Technical and Economic Feasibility of Treating Oilfield Produced Water to Create a 'New' Water Resource, Ground Water Protection Council Online, 2002; Available from: <http://www.gwpc.org>.
22. W.L. Bourcier, W.L., H. Brandt, and J.H. Tait, Pretreatment of Oil Field and Mine Waste Waters for Reverse Osmosis, in Produced Water 2 : Environmental Issues and Mitigation Technologies, M. Reed and S. Johnsen, Editors. Plenum Press, New York 1996.
23. A. Gorlov, A. Gorban, and V. Silantyev, Limits of Turbine Efficiency for Free Fluid Flow, *Journal of Energy Resources Technology* 123 (2001) 311-317.
24. C. Liu, J. Park, R. Migita, G. Qin, Experiments of a Prototype Wind-Driven Reverse Osmosis Desalination System with Feedback Control, *Desalination* 150 (2002) 277-287.

25. S.M. Habali and I.A. Saleh, Design of Stand-Alone Brackish Water Desalination Wind Energy System for Jordan, *Solar Energy* 52 (1994) 525-532.
26. L. Garcia-Rodriguez, V. Romero-Ternero, and C. Gomez-Camacho, Economic Analysis of Wind-Powered Desalination, *Desalination* 137 (2001) 259-265.
27. S.A. Kershman, J. Rheinlander, and H. Gabler, Seawater Reverse Osmosis Powered from Renewable Energy Sources - Hybrid Wind/Photovoltaic Grid Power Supply for Small-Scale Desalination in Libya, *Desalination* 153 (2002) 17-23.
28. The World Factbook: Field Listing - Exchange Rates. 2006, Central Intelligence Agency [accessed 2006 May 11]; Available from: <http://www.cia.gov/cia/publications/factbook/fields/2076.html>.
29. D. Weiner, D. Fisher, E. Moses, B. Katz, G. Maron, Operation Experience of a Solar- and Wind-Powered Desalination Demonstration Plant, *Desalination* 137 (2001) 7-13.
30. E.S. Mohamed and G. Papadakis, Design, Simulation and Economic Analysis of a Stand-Alone Reverse Osmosis Desalination Unit Powered by Wind Turbines and Photovoltaics, *Desalination* 164 (2004) 87-97.
31. M. Thomson and D. Infield, A Photovoltaic-Powered Seawater Reverse-Osmosis System Without Batteries, *Desalination* 153 (2003) 1-8.
32. M. Thompson, M.S. Miranda, and D. Infield, A Small-Scale Seawater Reverse-Osmosis System with Excellent Energy Efficiency Over a Wide Operating Range, *Desalination* 153 (2002) 229-236.
33. M.T. Rahbar, Improvement of the Design and Operation of Desalination Plants by Computer Modeling and Simulation, *Desalination* 92 (1993) 253-269.
34. W.L. Luyben, Dynamics and Control of Recycle Systems: 1. Simple Open-Loop and Closed-Loop Systems, *Industrial & Engineering Chemical Research* 32 (1993) 466.
35. W.L. Luyben, Use of Dynamic Simulation to Converge Complex Process Flowsheets, *Chemical Engineering Education* (2004) 142-149.
36. W. Driedger, Controlling Positive Displacement Pumps, *Hydrocarbon Processing* 75 (1996) 47-54.

37. M. Barrufet, D. Burnett, and B. Mareth. Modeling and Operation of Oil Removal and Desalting Oilfield Brines with Modular Units. in SPE Annual Technical Conference and Exhibition. 2005. Dallas, Texas, USA: Society of Petroleum Engineers.
38. R. Darby, Chemical Engineering Fluid Mechanics. 2nd ed., Marcel Dekker, New York, 2001.
39. M.S. Peters, K.D. Timmerhaus, and R.E. West, Plant Design and Economics for Chemical Engineers. 5th ed., McGraw-Hill, Boston, 2003.
40. A.C. Jimenez and K. Olson, Renewable Energy for Rural Health Clinics. National Renewable Energy Laboratory, U.S. Dept of Energy, Boulder, CO 1998.
41. Stand-Alone Photovoltaic Systems: A Handbook of Recommended Design Practices. Sandia National Laboratories, Albuquerque, N.M. 2003.
42. WinCAD Turbine Performance Model. Bergey Windpower Co., Norman, OK, 1997.
43. Wind - Average Speed (MPH). University of Utah [accessed 2005 December]; Available from: <http://www.met.utah.edu/jhorel/html/wx/climate/windavg.html>.
44. G.C. Vliet, Texas Solar Radiation Database (TSRDB), Journal of Solar Energy Engineering 126 (2004) 575-580.
45. E. Darton, Membrane Chemical Research: Centuries Apart, Desalination 132 (2000) 121-131.
46. Z. Amjad, Applications of Antiscalants to Control Calcium Sulfate Scaling in Reverse Osmosis Systems, Desalination 54 (1985) 263-276.
47. D. Hasson, A. Drak, and R. Semiat, Induction Times Induced in an RO System by Antiscalants Delaying CaSO<sub>4</sub> Precipitation, Desalination 157 (2003) 193-207.
48. R. Carnahan, L. Bolin, and W. Suratt, Biofouling of PVD-1 Reverse Osmosis Elements in the Water Treatment Plant of the City of Dunedin, Florida, Desalination 102 (1995) 235-244.
49. J. Baker and L. Dudley, Biofouling in Membrane Systems - A Review, Desalination 118 (1998) 81-90.

50. H. Flemming, G. Schaule, T. Grieb, J. Schmitt, A. Tamachkiorowa, Biofouling—the Achilles Heel of Membrane Processes, *Desalination* 113 (1997) 215-225.
51. D. van der Kooij, H. Vrouwenvelder, and H.R. Veenendaal, Elucidation and Control of Biofilm Formation Processes in Water Treatment and Distribution Using the Unified Biofilm Approach, *Water Science and Technology* 47 (2003) 83-90.
52. T. Griebe and H. Flemming, Biocide-free Antifouling Strategy to Protect RO Membranes from Biofouling, *Desalination* 118 (1998) 235-244.
53. Texas Renewable Energy Resources: Solar. Texas State Energy Conservation Office [accessed 2006 April 20]; Available from: <http://www.infinitepower.org/ressolar.htm>.

## APPENDIX A

### MEMBRANE FOULING PREVENTION AND TREATMENT

#### Scaling Prediction

When a reverse osmosis membrane is in operation, normalized flux decline is the usual indicator of fouling. Obviously, it is much preferable to avoid the scaling in the first place, and for this reason an accurate scaling prediction method is desirable.

Many efforts have been made to that end. In the case of calcium carbonate scaling, a simple, widely-used predictor is the Langelier Saturation Index (LSI).

$$\text{LSI} = \text{pH}_c - \text{pCa} + \text{pAlk} + \text{K}$$

where:

$\text{pH}_c$  = pH of the concentrate stream

$\text{pCa}$  = negative logarithm of calcium concentration

$\text{pAlk}$  = negative logarithm of alkalinity ( $\{\text{CO}_3^{2-}\}$  and  $\{\text{HCO}_3^-\}$ )

$\text{K}$  = a constant which depends on ionic strength and temperature

For hand calculations, values for  $\text{K}$  can be obtained from the appropriate nomograph. An LSI value of 0 indicates the threshold of precipitation, with positive values indicating, precipitation and scaling potential. The LSI was modified by Stiff and Davis for application to oilfield produced waters. The method for determining S&DSI is the same as described above for LSI, differing only in the values of  $\text{K}$ .

Estimating sulfate scaling potential is straightforward as well. The ion product for the various sulfate salts are calculated, then compared with the appropriate solubility product value. Some membrane manufacturers, such as DuPont, provide figures within their technical manuals from which solubility constants are plotted as functions of ionic strength and/or temperature.

In the case of silica, the following formula is recommended by DuPont to predict maximum permissible silica concentration:



$$\text{SiO}_{2,\text{max}} = \text{SiO}_{2,\text{temp}} \times \text{pH correction factor}$$

where:

$\text{SiO}_{2,\text{max}}$  = maximum concentrate stream silica, mg/l

$\text{SiO}_{2,\text{temp}}$  = silica solubility conc. at pH 7.5 as a function of temperature, mg/l

pH correction factor = silica solubility factor at system pH

The  $\text{SiO}_{2,\text{temp}}$  and pH correction factors can be found from charts on which they are plotted versus temperature and brine pH, respectively [16].

### Scaling Prevention

Mineral scaling is perhaps the most controllable of the fouling phenomena. Four options available to prevent it are [16],[19]:

- 1) removal of the responsible ion(s) in pretreatment
- 2) pH adjustment
- 3) reducing system recovery
- 4) inhibition of crystal growth

The method of ion removal depends on the species targeted for removal. Lime softening can reduce both calcium ion and silica concentrations, while ions exchange is another option for  $\text{Ca}^{2+}$  removal [16]. In small-scale systems, the additionally capital costs associated with lime softening and ion exchange often render them impractical, but they are not uncommon in large, municipal installations.

pH adjustment may be the simplest option for plants with high silica or  $\text{CaCO}_3$  scaling potential. Reducing pH increases  $\text{CaCO}_3$  solubility, but decreases silica solubility, so in a system in which both species threaten precipitation, pH adjustment would not be suitable. Also, while sulfuric acid is most frequently used to lower feedwater pH, another acid such as HCl must be used if sulfate scaling is a potential problem.

Reduction of water recovery lowers scaling occurrence in membrane systems simply because the degree of saturation of the various minerals is reduced. System economics dictate whether lowering recovery is preferable to other preventative options for a particular plant.

Scale inhibiting chemicals, the fourth method of scale prevention, are available for all of the major scaling species and are in wide use throughout the reverse osmosis industry. They work by interfering with one or more steps of the crystallization mechanism. “Threshold inhibitors” disrupt the clustering process. “Crystal distortion” inhibitors interfere with crystal growth, such that a weak, irregular structure is formed that does not tend to attach to the RO membrane. Low molecular weight (<5000) polymers can function in this fashion. “Dispersion” inhibitors are high molecular weight (>20000) polymers that prevent scaling by chemisorbing to the surface of small crystals, giving them a surface charge which causes them to repel other crystals, limiting crystals to a less-harmful size. Finally, chelating agents can operate as inhibitors by solubilising precipitated particles [45]. Table 9 summarizes three major classes of scale inhibitors.

**Table 9. Scale Inhibitors**

Inhibitor	Description
Sodium hexametaphosphate (NaPO <sub>3</sub> ) <sub>6</sub>	First widely-used chemical inhibitor. Can undergo hydrolytic cleavage of the O-P-P group, which can lead to formation of calcium phosphate scale.
Phosphonate compounds (many varieties) O <sub>3</sub> P – C group	Similar performance to SHMP, but without the risk of cleavage and subsequent phosphate scale formation.
Polyacrylic acid [CH <sub>2</sub> -CH-COOH] <sub>n</sub>	Can function as threshold, crystal distorting, or dispersion inhibitor, depending on polymer’s molecular weight.

A 1985 study by Amjad [46] indicated a significant difference in the effectiveness of various inhibitors on calcium sulfate scale suppression. The relative effectiveness was given as: formulated polyelectrolyte > polyacrylate > hexametaphosphate >> pyrophosphate ≈ tripolyphosphate ≈ polystyrene sulfonate ≈ polyacrylamide ≈ control (no antiscalant). Hasson [47] found similar results in a 2003 study of antiscalants’ effects on CaSO<sub>4</sub> induction times. While polyelectrolytes were not tested, SHMP and polyacrylate were the top performers in his study.

## **Biofouling Prevention and Treatment**

In terms of control biofouling by means of adjusting plant operating parameters, the only parameter that affects biological growth is water recovery. Operating at low recovery reduces the rate of nutrient passage into the biofilm, slowing growth. Also, greater axial flow in low-recovery systems results in higher shear which tends to limit the thickness of the layer [48]. However, system economics obviously favor high recovery rates, so controlling biofouling by lowering recovery is not usually practical.

The most common approach to overcoming biofouling is through the use of biocides [20]. Biocides may be classified as either oxidizing or non-oxidizing. Oxidizing biocides include chlorine, bromine, chloramines, hydrogen peroxide, ozone, and more. Since many membranes are susceptible to damage by strong oxidants, their use requires application of a pretreatment dose to kill the organisms, followed by an oxidant removal step to prevent it from reaching the membrane. Sodium bisulphate is the agent commonly used to remove residual chlorine.

There is some debate as to whether chlorine is effective in reducing biofouling in membrane systems. In fact, some experiences show chlorine may have the opposite of the intended effect. For example, a Mediterranean Sea hollow-fiber RO plant experienced reduced biofouling when it ceased use of chlorine in pretreatment. Several factors may contribute to this result.

- Surviving bacteria may produce more EPS as a defense against the treatment, thickening the biofoulant layer

- Organisms killed by the oxidation treatment may serve as an additional food source for microorganisms in the existing biofilm

- Chlorination may decompose humic acids into smaller compounds, providing additional nutrition to existing biofilm inhabitants

Several non-oxidizing biocides are also available, such as formaldehyde, glutaraldehyde, and quaternary ammonium compounds, none of which are suitable for potable water applications. Many proprietary biocides are available in the marketplace as well, some of which are approved for potable use. A difficulty often encountered by users of these products is the development of immunity in the microorganisms. To reduce this possibility, plants personnel should apply a “shock dose” (high dose for a

short duration) strategy rather than a continual low dose. Alternating between two biocides may help as well. The second biocide will likely kill those organisms that happened to be resistant to the first [49].

In recent years, researchers have begun to explore biofiltration as a pretreatment to inhibit biofilm formation in membrane systems. The concept is to employ biologically-active media in pretreatment to consume organic matter. The reduced downstream availability of organic matter should slow growth of microorganisms on the membranes due to a lack of nutrition. Flemming et al. [50] describes this concept as a “bioreactor in the right place,” contrasted with a biofouled membrane which would constitute a bioreactor in the wrong place.

Slow sand filtration is one method of incorporating biofiltration into a water treatment train. Microbial life flourishes in sand beds. In a study by van der Kooij and Vrouwenvelder [51], an RO plant with slow sand filtration pretreatment was compared to two other plants that lacked biofiltration. The former plant showed lower levels of fouling than the latter two.

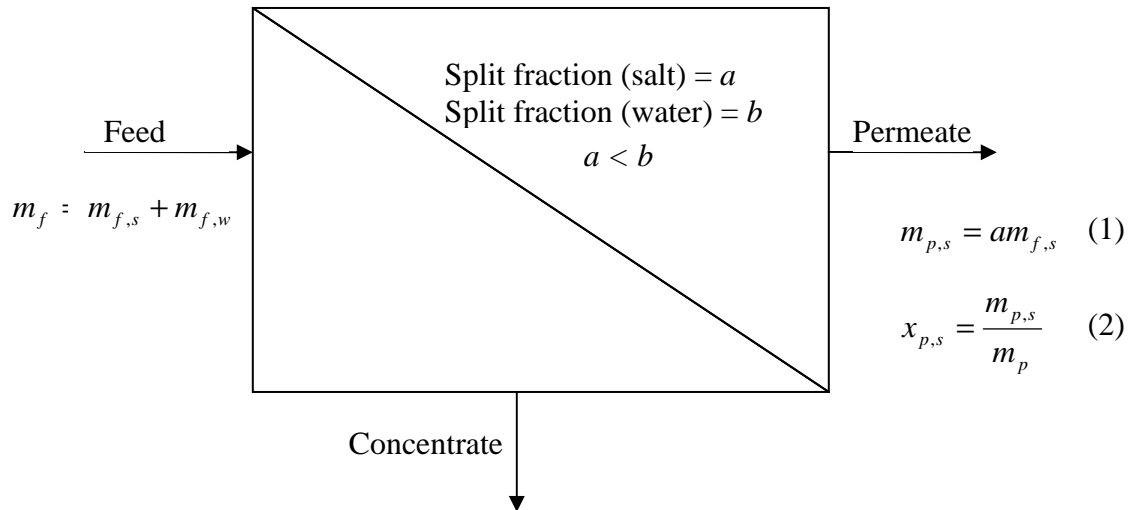
Griebe [52] also studied sand biofilter use to control levels of nutrients and thus biofilm growth in cross-flow membranes. His apparatus lowered levels of biodegradable dissolved organic carbon (BDOC) in plant feedwater from 1.22 mg/l to 0.12. He stated that the threshold level of BDOC to prevent biofilm from progressing to biofouling was about 0.1 mg/l.

A second approach has been developed in Europe over the last 25 years, chiefly for drinking water treatment applications. Biologically active carbon is obtained by allowing granulated active carbon filters to saturate with organic matter, making them havens for microbes that consume the types of matter that have accumulated on the filter (and thus occur in the feedwater). It is reported that such filters remove 5-75% of Total Organic Carbon.

## APPENDIX B

### MATERIAL BALANCE AROUND RO MEMBRANE

The purpose of carrying out the following balance was to relate an Aspen Dynamics input parameter (salt split fraction) to the membrane empirical model's corresponding parameter, Solute Rejection.



Definition of Salt/Solute Rejection: 
$$R = 1 - \frac{x_{p,s}}{x_{f,s}} \quad (3)$$

From (1), (2), (3),

$$a = \frac{m_{p,s}}{m_{f,s}} = \frac{x_{p,s} m_p}{m_{f,s}} = \frac{(1-R)x_{f,s} m_p}{m_{f,s}}$$

Where:

$m_p$  = permeate stream mass flow rate

$m_{p,s}$  = mass flow of salt in permeate stream

$m_{f,s}$  = mass flow of salt in feed stream

$x_{p,s}$  = mass fraction of salt in permeate stream

$x_{f,s}$  = mass fraction of salt in feed stream

## APPENDIX C

### COMPUTER CODE

#### ROsimulator Task

Task ROsimulator runs before step

//Units: Pressure in Bar, Flow in Cubic Meters per Hour

//Model Bounds

If  $14 < \text{BLOCKS}(\text{"MIXR"}).P$  and  $83 > \text{BLOCKS}(\text{"MIXR"}).P$  and  
 $\text{STREAMS}(\text{"SEPIN"}).Fv > 1.3$  and  $\text{STREAMS}(\text{"SEPIN"}).Fv < 3$  Then

//Pressure Drop

$\text{BLOCKS}(\text{"SEPA"}).P\_drop(\text{"CONC1"}): \text{STREAMS}(\text{"SEPIN"}).Fv / 1.363 * (1.0976 - 0.903 * \text{BLOCKS}(\text{"SEPA"}).fsplt(\text{"PROD"}));$

//Permeate Split Fraction

$\text{BLOCKS}(\text{"SEPA"}).fsplt(\text{"PROD"}): ((3.8444 * ((\text{BLOCKS}(\text{"MIXR"}).P - \text{BLOCKS}(\text{"SEPA"}).P\_drop(\text{"CONC1"}) / 2) * 14.5 / (\text{STREAMS}(\text{"SEPIN"}).Fv * 90.58))^{1.0425} + 0.6099 * (\text{STREAMS}(\text{"SEPIN"}).Zmn(\text{"SODIU-01"}) * 1000000 / ((\text{BLOCKS}(\text{"MIXR"}).P - \text{BLOCKS}(\text{"SEPA"}).P\_drop(\text{"CONC1"}) / 2) * 14.5))^{-0.3133} - 0.0271 * (\text{STREAMS}(\text{"SEPIN"}).Zmn(\text{"SODIU-01"}) * 1000000 / (\text{STREAMS}(\text{"SEPIN"}).Fv * 90.58))^{1.0963}) / 100;$

//Salt Rejection

$\text{BLOCKS}(\text{"SEPA"}).sfrac(\text{"CONC1"}, \text{"SODIU-01"}): 1 - \text{STREAMS}(\text{"SEPIN"}).Zmn(\text{"SODIU-01"}) * \text{BLOCKS}(\text{"SEPA"}).fsplt(\text{"PROD"}) * \text{STREAMS}(\text{"SEPIN"}).Fm * (1 - ((99.9901 * ((\text{BLOCKS}(\text{"MIXR"}).P - \text{BLOCKS}(\text{"SEPA"}).P\_drop(\text{"CONC1"}) / 2) * 14.5 / (\text{STREAMS}(\text{"SEPIN"}).Fv * 90.58))^{-0.0013} - 0.0045 * (\text{STREAMS}(\text{"SEPIN"}).Zmn(\text{"SODIU-01"}) * 1000000 / ((\text{BLOCKS}(\text{"MIXR"}).P - \text{BLOCKS}(\text{"SEPA"}).P\_drop(\text{"CONC1"}) / 2) * 14.5))^{1.6575} + 0.000009357 * (\text{STREAMS}(\text{"SEPIN"}).Zmn(\text{"SODIU-01"}) * 1000000 / (\text{STREAMS}(\text{"SEPIN"}).Fv * 90.58))^{2.071}) / 100) / \text{STREAMS}(\text{"SEPIN"}).Fmcn(\text{"Sodiu-01"});$

//No separation if conditions are outside of model bounds

Else

$\text{BLOCKS}(\text{"SEPA"}).fsplt(\text{"PROD"}): 0;$

EndIf

Restart after 0.05;

End

## Renewable Energies Spreadsheet Tool

Option Explicit

Sub OtherLocation()

    If Range("B6").Value = "other" Then frmLocation.Show  
    BattStorAndDesCurr

End Sub

Sub OtherBattery()

    If Range("B23").Value = "other" Then frmBattery.Show Else Batteries

End Sub

Sub OtherPV()

    If Range("B34").Value = "other" Then FrmPV.Show Else Solar

End Sub

Sub BattStorAndDesCurr()

    Dim Days, PeakSun, Wind, WindA, WindM, SunA, SunM, Weibull, Altitude, Energy  
    As Double

    Dim MyRow, MyColumn, i As Integer

    If Range("B6").Value = "other" Then GoTo Jump

    'getting city and availability and assigning matrix address

    For i = 1 To 6

        If Range("B6").Value = Sheet3.Range("B17").Offset(i, 0) Then MyRow = i

    Next i

    If Range("B22").Value = "0.95" Then MyColumn = 1

    If Range("B22").Value = "0.99" Then MyColumn = 2

    'filling in location-appropriate wind/sun values

    WindA = Sheet3.Range("B17").Offset(MyRow, 4).Value

```

WindM = Sheet3.Range("B17").Offset(MyRow, 3).Value
SunA = Sheet3.Range("B17").Offset(MyRow, 6).Value
SunM = Sheet3.Range("B17").Offset(MyRow, 5).Value

```

```

Range("B8").Value = WindA
Range("B9").Value = WindM
Range("B10").Value = SunA
Range("B11").Value = SunM

```

```

'getting Days value from other sheet, then putting into _
appropriate cell on current sheet
Days = Sheet3.Range("B17").Offset(MyRow, MyColumn).Value
Range("F22").Value = Days

```

```

'getting Altitude, Weibull data for selected city
Altitude = Sheet3.Range("B17").Offset(MyRow, 7).Value
Weibull = Sheet3.Range("B17").Offset(MyRow, 8).Value

```

```

'pasting Altitude and Weibull into turbine model
Sheet4.Range("B11").Value = Weibull
Sheet4.Range("B12").Value = Altitude

```

```

'getting appropriate insolation then Design Current Calculation
Jump:

```

```

If Range("B7").Value = "Annual Average Properties" Then
PeakSun = Range("B10").Value
Wind = Range("B8").Value
End If

```

```

If Range("B7").Value = "Lowest Monthly Average Properties" Then
PeakSun = Range("B11").Value
Wind = Range("B9").Value
End If

```

```

Range("F17").Value = Range("F15").Value / PeakSun

```

```

'pasting Wind into turbine model
Sheet4.Range("B10").Value = Wind
Sheet4.Range("B17").Value = 1 - Range("B44").Value

```

```

'pasting energy value from turbine model to worksheet
Energy = Sheet4.Range("G13").Value
Range("F44").Value = Energy

```

```

End Sub

```



Sub Solar()

```
Dim Current, Voltage, Weight, Area, Cost As Double
Dim MyRow, i As Integer
Dim Name As String
```

```
'getting make/model and assigning matrix address
```

```
For i = 1 To 5
```

```
    If Range("B34").Value = Sheet3.Range("B31").Offset(i, 0) Then MyRow = i
Next i
```

```
If MyRow < 5 Then
```

```
'reading appropriate values from other sheet
```

```
Current = Sheet3.Range("B31").Offset(MyRow, 1).Value
Voltage = Sheet3.Range("B31").Offset(MyRow, 2).Value
Weight = Sheet3.Range("B31").Offset(MyRow, 3).Value
Area = Sheet3.Range("B31").Offset(MyRow, 4).Value
Cost = Sheet3.Range("B31").Offset(MyRow, 7).Value
```

```
'pasting values onto current sheet
```

```
Range("B35").Value = Current
Range("B36").Value = Voltage
Range("B37").Value = Weight
Range("B38").Value = Area
Range("B39").Value = Cost
```

```
End If
```

End Sub

Sub Batteries()

```
Dim i, MyRow, Voltage As Integer
Dim Cost, Capacity, Weight As Double
```

```
For i = 1 To 5
```

```
    If Range("B23").Value = Sheet3.Range("B40").Offset(i, 0) Then MyRow = i
Next i
```

```
If MyRow < 5 Then
```

```
Voltage = Sheet3.Range("B40").Offset(MyRow, 1).Value
Capacity = Sheet3.Range("B40").Offset(MyRow, 2).Value
Weight = Sheet3.Range("B40").Offset(MyRow, 3).Value
```

```
Cost = Sheet3.Range("B40").Offset(MyRow, 4).Value
```

```
Range("B24").Value = Voltage
```

```
Range("B25").Value = Capacity
```

```
Range("B26").Value = Weight
```

```
Range("B27").Value = Cost
```

```
End If
```

```
End Sub
```

```
Private Sub Worksheet_Change(ByVal Target As Range)
```

```
    If (Target.Column = 2) And (Target.Row = 6) Then OtherLocation
```

```
    If (Target.Column = 2) And (Target.Row = 23) Then OtherBattery
```

```
    If (Target.Column = 2) And (Target.Row = 34) Then OtherPV
```

```
    If (Target.Column = 2) And ( _
```

```
        (Target.Row = 7) Or _
```

```
        (Target.Row = 15) Or _
```

```
        (Target.Row = 16) Or _
```

```
        (Target.Row = 17) Or _
```

```
        (Target.Row = 18) Or _
```

```
        (Target.Row = 22) Or _
```

```
        (Target.Row = 44)) _
```

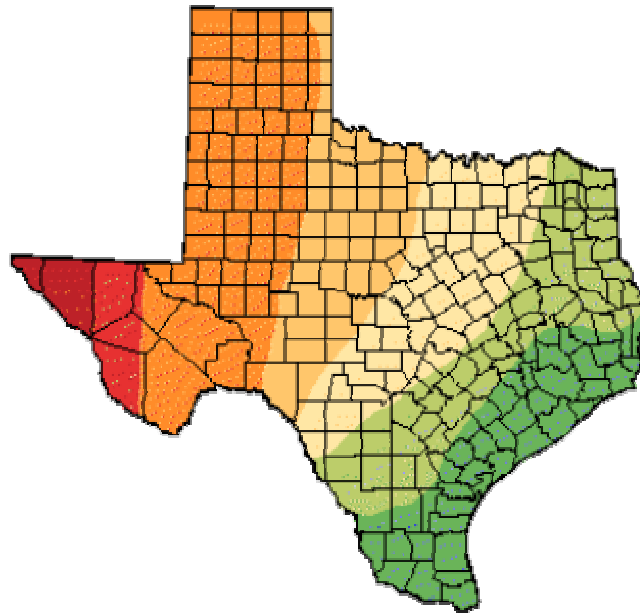
```
    Then
```

```
        BattStorAndDesCurr
```



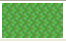







```
    End If
```

```
End Sub
```

**APPENDIX D**  
**RENEWABLE ENERGY RESOURCE MAPS**



**Figure 19. Texas Solar Resource Map [53]**

AVERAGE DIRECT NORMAL INSOLATION MAP LEGEND			
COLOR KEY	per day (kWh/m <sup>2</sup> -day)	per YEAR	
		(MJ/m <sup>2</sup> )	(quads/100 mi <sup>2</sup> )
	<3.0	<3,940	<1.0
	3.0 - 3.5	3,940 - 4,600	1.0 - 1.1
	3.5 - 4.0	4,600 - 5,260	1.1 - 1.3
	4.0 - 4.5	5,260 - 5,910	1.3 - 1.5
	4.5 - 5.0	5,910 - 6,570	1.5 - 1.6
	5.0 - 5.5	6,570 - 7,230	1.6 - 1.8
	5.5 - 6.0	7,230 - 7,880	1.8 - 1.9
	6.0 - 6.5	7,880 - 8,540	1.9 - 2.1
	6.5 - 7.0	8,540 - 9,200	2.1 - 2.3
	>7.0	>9,200	>2.3

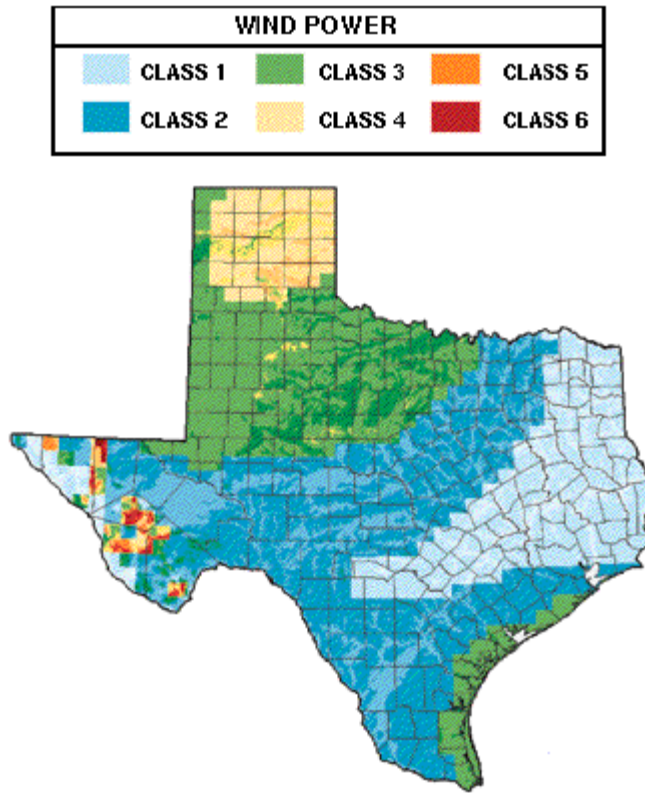


Figure 20. Texas Wind Speed Map [6]

**VITA**

Name: Brett Mareth

Address: 6642 Theda, Corpus Christi, TX 78412

Email Address: bmareth@tamu.edu

Education: B.S., Chemical Engineering, Texas A&M University, 2003  
M.S., Chemical Engineering, Texas A&M University, 2006